NASA/TM—2011-217006

DBD Plasma Actuators for Flow Control in Air Vehicles and Jet Engines—Simulation of Flight Conditions in Test Chambers by Density Matching

David E. Ashpis
Glenn Research Center, Cleveland, Ohio

Douglas R. Thurman
U.S. Army Research Laboratory, Glenn Research Center, Cleveland, Ohio

March 2011

NASA STI Program . . . in Profile

Since its founding, NASA has been dedicated to the advancement of aeronautics and space science. The NASA Scientific and Technical Information (STI) program plays a key part in helping NASA maintain this important role.

The NASA STI Program operates under the auspices of the Agency Chief Information Officer. It collects, organizes, provides for archiving, and disseminates NASA's STI. The NASA STI program provides access to the NASA Aeronautics and Space Database and its public interface, the NASA Technical Reports Server, thus providing one of the largest collections of aeronautical and space science STI in the world. Results are published in both non-NASA channels and by NASA in the NASA STI Report Series, which includes the following report types:

- TECHNICAL PUBLICATION. Reports of completed research or a major significant phase of research that present the results of NASA programs and include extensive data or theoretical analysis. Includes compilations of significant scientific and technical data and information deemed to be of continuing reference value. NASA counterpart of peer-reviewed formal professional papers but has less stringent limitations on manuscript length and extent of graphic presentations.

- TECHNICAL MEMORANDUM. Scientific and technical findings that are preliminary or of specialized interest, e.g., quick release reports, working papers, and bibliographies that contain minimal annotation. Does not contain extensive analysis.

- CONTRACTOR REPORT. Scientific and technical findings by NASA-sponsored contractors and grantees.

- CONFERENCE PUBLICATION. Collected papers from scientific and technical conferences, symposia, seminars, or other meetings sponsored or cosponsored by NASA.

- SPECIAL PUBLICATION. Scientific, technical, or historical information from NASA programs, projects, and missions, often concerned with subjects having substantial public interest.

- TECHNICAL TRANSLATION. English-language translations of foreign scientific and technical material pertinent to NASA's mission.

Specialized services also include creating custom thesauri, building customized databases, organizing and publishing research results.

For more information about the NASA STI program, see the following:

- Access the NASA STI program home page at *http://www.sti.nasa.gov*

- E-mail your question via the Internet to *help@sti.nasa.gov*

- Fax your question to the NASA STI Help Desk at 443–757–5803

- Telephone the NASA STI Help Desk at 443–757–5802

- Write to:
  NASA Center for AeroSpace Information (CASI)
  7115 Standard Drive
  Hanover, MD 21076–1320

NASA/TM—2011-217006

DBD Plasma Actuators for Flow Control in Air Vehicles and Jet Engines—Simulation of Flight Conditions in Test Chambers by Density Matching

David E. Ashpis
Glenn Research Center, Cleveland, Ohio

Douglas R. Thurman
U.S. Army Research Laboratory, Glenn Research Center, Cleveland, Ohio

National Aeronautics and
Space Administration

Glenn Research Center
Cleveland, Ohio 44135

March 2011

Acknowledgments

This project was supported by the NASA Subsonic Fixed Wing Project of the Fundamental Aeronautics Program. We wish to thank Scott Jones and Michael Tong from NASA Glenn Research Center for their help in developing the engine models. Thanks also to Mikhail Shneider (Princeton University), Andrey Starikovskiy (Princeton University), and Alex Likhanskii (Tech-X Corporation) for useful discussions. Thanks for NASA Glenn Publishing department—Nancy Mieczkowski for the graphics, Lisa Greeney for layout, and Mary Eitel-Kim for coordinating production of this report.

This report contains preliminary findings, subject to revision as analysis proceeds.

This work was sponsored by the Fundamental Aeronautics Program at the NASA Glenn Research Center.

Level of Review: This material has been technically reviewed by technical management.

Available from

NASA Center for Aerospace Information
7115 Standard Drive
Hanover, MD 21076–1320

National Technical Information Service
5301 Shawnee Road
Alexandria, VA 22312

Available electronically at http://www.sti.nasa.gov

DBD Plasma Actuators for Flow Control in Air Vehicles and Jet Engines—Simulation of Flight Conditions in Test Chambers by Density Matching

David E. Ashpis
National Aeronautics and Space Administration
Glenn Research Center
Cleveland, Ohio 44135

Douglas R. Thurman
U.S. Army Research Laboratory
Glenn Research Center
Cleveland, Ohio 44135

Abstract

Dielectric Barrier Discharge (DBD) Plasma actuators for active flow control in aircraft and jet engines need to be tested in the laboratory to characterize their performance at flight operating conditions. DBD plasma actuators generate a wall-jet electronically by creating weakly ionized plasma, therefore their performance is affected by gas discharge properties, which, in turn, depend on the pressure and temperature at the actuator placement location. Characterization of actuators is initially performed in a laboratory chamber without external flow. The pressure and temperature at the actuator flight operation conditions need to be simultaneously set in the chamber. A simplified approach is desired. It is assumed that the plasma discharge depends only on the gas density, while other temperature effects are assumed to be negligible. Therefore, tests can be performed at room temperature with chamber pressure set to yield the same density as in operating flight conditions.

The needed chamber pressures are shown for altitude flight of an air vehicle and for jet engines at sea-level takeoff and altitude cruise conditions. Atmospheric flight conditions are calculated from standard atmosphere with and without shock waves. The engine data was obtained from four generic engine models; 300-, 150-, and 50-passenger (PAX) aircraft engines, and a military jet-fighter engine. The static and total pressure, temperature, and density distributions along the engine were calculated for sea-level takeoff and for altitude cruise conditions. The corresponding chamber pressures needed to test the actuators were calculated. The results show that, to simulate engine component flows at in-flight conditions, plasma actuator should be tested over a wide range of pressures. For the four model engines the range is from 12.4 to 0.03 atm, depending on the placement of the actuator in the engine. For example, if a DBD plasma actuator is to be placed at the compressor exit of a 300 PAX engine, it has to be tested at 12.4 atm for takeoff, and 6 atm for cruise conditions. If it is to be placed at the low-pressure turbine, it has to be tested at 0.5 and 0.2 atm, respectively. These results have implications for the feasibility and design of DBD plasma actuators for jet engine flow control applications. In addition, the distributions of unit Reynolds number, Mach number, and velocity along the engine are provided. The engine models are non-proprietary and this information can be used for evaluation of other types of actuators and for other purposes.

Introduction

There is strong interest in active flow control techniques for applications in air vehicles as well as in jet engines, for example, to eliminate flow separation, improve efficiency or reduce noise (Ref. 1). Dielectric Barrier Discharge (DBD) Plasma actuators were proposed for active flow control of various flows, and the technology has been an active research area in the last decade.

The main active flow control technique in aerodynamics is based on injection of small jets in a steady or unsteady manner into the flow. The small input creates a large global effect that provides the desired flow improvement. DBD plasma actuators create a wall-jet by purely electronic means. The jet can be steady, or in unsteady mode by pulsing or modulating, and can be used for active flow control, similar to any pneumatically- or mechanically-generated jet.

A DBD actuator is shown in Figure 1. The actuator consists of a pair of thin conducting electrodes separated by a dielectric. Usually there is one exposed electrode and one covered electrode and the electrodes are offset. Typically, at atmospheric conditions, a high voltage (1 to 40 kV RMS), high frequency (1 to 20 kHz), signal is applied to the electrodes, creating localized weakly ionized gas plasma discharge on the surface near the edge of the exposed electrode. A typical discharge is shown in Figure 2.

The jet is generated in the plasma region via the electrohydrodynamic effect, a process of collisions between ions and neutral molecules in the plasma. The actuator construction is very simple, but the physical mechanisms involved are quite complex and include interactions among electrical fields, electrons, positively and negatively charged species, the electrodes, and the dielectric surface (Refs. 2 to 4). Gas is drawn from the surroundings to form a thin wall jet that is roughly parallel to the surface and directed away from the exposed electrode edge in the direction of the covered electrode, as visualized by experiments and computation (Refs. 5 to 7). There is slight heating involved, but its effect on the jet is negligible. Other types of plasma-based flow control devices that generate localized intense heating (Ref. 8) are not included in the scope of devices addressed in this paper. More detailed information and references on DBD actuators and their applications for aerodynamic flow control can be found in several review articles (Refs. 9 to 12).

The advantages of DBD actuators are that they are surface-mounted, fully electronic, low power, high frequency-band devices. There are no moving parts, tubes, ducts or surface holes. Flexible operation is possible by controlling the input voltage and waveforms. DBD plasma actuators are particularly attractive for gas turbine and turbomachinery applications: They are thin, surface mounted, and do not require internal volumes or passages. Their construction can be made suitable for high temperature environment by choosing high-temperature alloys for the electrodes and temperature-resistant ceramic materials for the dielectric. They can easily be integrated with futuristic engine components to be made of ceramics and composites.

The majority of the research in DBD actuators area was focused on applications in external flows, particularly for wings and airframes, rather than on propulsion. But there have been important efforts directed to turbomachinery applications. There have been several successful experimental demonstrations of active flow control with DBD plasma actuators to eliminate low Reynolds number separation in Low-Pressure Turbine flows (Refs. 13 to 16), and to reduce effects of turbine tip leakage (Refs. 17 to 20). Those experiments were performed in wind tunnels or linear cascades at room temperature.

DBD actuators need to be tested in actual flight conditions in order to be used as flow control devices in practical applications. Some flight tests were performed on air vehicles; on a small remotely controlled airship (Refs. 21 and 22) a full-size piloted glider (Ref. 23), and a small UAV (Ref. 24), but no tests have been performed in jet engines. The aerodynamic performance of the actuators needs to be characterized to prove that they have sufficient authority at the flow conditions at the location of their placement in the air vehicle or jet engine. In addition, the electrical performance, particularly the power consumption of the actuators, needs to be quantified, as it is needed for design of power supplies and for cost-benefit analysis of the flow control technology. This paper addresses the test conditions needed to characterize the actuators in the laboratory.

The basic characterization in the laboratory is performed without external flow. The aerodynamic performance is characterized by measuring the velocity profile of the wall jet and/or the thrust generated by the actuator. The electrical performance is characterized by measuring the current, voltage, and power. Most of the tests to date have been performed at room temperature and atmospheric conditions, but in order to simulate flight conditions the actuator has to be placed in a chamber with controlled temperature and pressure representative of the flow conditions in flight. A small number of tests are reported in the literature in chambers at room temperature and sub-atmospheric conditions, with some conflicting results

(Refs. 25 to 32). Tests at atmospheric altitude conditions have been performed in an environmental chamber (Ref. 33), where temperature and pressure were varied simultaneously. These tests were mostly motivated by external aerodynamics applications. Tests at above-atmospheric pressures at room temperature were reported in References 34 and 35, and provide information relevant to internal flow applications.

The actuator performance has to be tested in conditions that simulate the operating conditions in flight, at the location where the actuator is placed. The applications in the jet engine are particularly challenging because of the high temperatures and high pressure ratios in several engine components. It is desirable to find a simpler approach to eliminate this technical complication. The question that arises is how to simulate the conditions in an operating jet engine in order to test the actuators properly. Because the principle of operation of DBD actuators depend on electrical discharges and on the associated force generation mechanisms, the performance of the actuator will be affected by the pressure, temperature and properties of the gas. It is assumed that for the range of temperatures in atmospheric flight and in the jet engine, the gas density alone is the significant gas property influencing the performance of the actuator. Therefore the flight conditions can be simulated by matching the density in the laboratory. It is a simple idea that has not been proposed before.

The outline of this paper is as follows. After addressing a relatively simple case of an air vehicle flying at altitude, attention is focused on the jet engine applications. First, information is provided on pressure, temperature, density, unit Reynolds number, Mach number, and velocity distribution along the flow-path of four thrust classes of jet engines. This information is derived from non-proprietary engine models used in system analysis studies by NASA. These models include cycle, flow path and sizing. Then, by setting the chamber pressure at room temperature, the density is matched to the in-flight operating conditions. The range of the needed chamber pressures was calculated using ideal gas law, by matching the flow densities. It depends on the placement of the actuator, and the results are presented for the four engine classes at takeoff and cruise conditions. This information is useful as a guideline for testing requirements of DBD plasma actuators at engine flight conditions. The engine information documented here, which is often hard to find in publically available sources, is useful for evaluation of other types of actuators as well as for other purposes.

Nomenclature

H	Altitude
M	Mach number
P	Static pressure
R	Gas constant
Rey	Reynolds number
T	Static temperature
V	Velocity
X	Axial distance along the engine
ρ	Density

Subscripts:

c	Conditions in chamber

Acronyms:

DBD	Dielectric Barrier Discharge
HPC	High pressure Compressor
HPT	High pressure Turbine

LPC Low Pressure Compressor
LPT Low Pressure Turbine
PAX Passengers

Jet Engine Data Source—Engine Models

The engine models used in this study were developed based on information available in open literature and empirical estimates. Cycle analysis was performed with the Numerical Propulsion Simulation System (NPSS) code (Refs. 36 and 37), providing performance parameters such as thrust, component pressure ratios, and velocities, temperatures, and pressures at each engine station. Aeromechanical analysis and estimates of engine and component weights were calculated using the Weight Analysis of Turbine Engines (WATE) code (Ref. 38), which also provides a flow path schematic of the engine. Generic engine models representing four different thrust classes were developed: 300-, 150- and 50-passenger (PAX) aircraft engines, and a military jet-fighter engine. These models are a good representation of actual engines. Note that the 150 PAX model is a conceptual design of a generic geared high bypass turbofan. The primary engine parameters of thrust, weight, overall pressure ratio, and bypass ratio are listed in Table 1 and the schematic of each engine is shown in Figure 3. The axial coordinates of the components outflow stations are listed in Table 2.

Engine conditions were calculated at the inlet and exit flow stations of the various engine components. Data was acquired for two engine operating conditions: sea-level takeoff and altitude cruise at 35,000 ft. Data for the 50 PAX engine is also shown for an additional cruise altitude of 65,000 ft, as this type of engine is also used for high-flying air vehicles. Figures 4 to 7 show the following parameters for each engine: static and total (stagnation) pressure, temperature, and density, as well as unit Reynolds number, Mach number and velocity. Ideal gas conditions were assumed. For all data shown, the flights Mach numbers are, M = 0.8 at cruise, and M = 0 at takeoff. Figure 6(d2) for the 50 PAX engine also shows cruise Mach numbers of M = 0.5, 0.6, and 0.8 at altitude of 65,000 ft.

There is more data presented than is strictly needed for development of the subject test conditions. The motivation for including the extra data is to make it available to the research community because it is hard to find non-proprietary actual engine data. The engine data presented here is unrestricted and can be used for other purposes.

Test Conditions for DBD Plasma Actutors

Several assumptions are used to develop the test conditions in laboratory experiments in quiescent environment (no flow) in a chamber:

(a) The effect of temperature and pressure on plasma kinetics and chemistry is ignored. This assumption is reasonable for the range of temperatures in the jet engines, and is further discussed below.

(b) The effect of temperature on the electrical properties of the actuator, particularly on the capacitance of the dielectric, is negligible. The capacitance variation was calculated in Reference 33, and was shown to be small.

(c) Actuator heat generation is negligible. This assumption is based on experimental observations for the range of power and voltages applied to conventional DBD plasma actuators.

(d) Gas composition effects are ignored. There is a small effect of the composition of the atmosphere variation with altitude mainly due to variation of the oxygen/nitrogen ratio (Ref. 32). Potentially there may be an effect due to the presence of combustion products in the areas of the engine downstream of the combustors. For simplicity these effects are assumed to be insignificant.

(e) Gas thermodynamic properties are constant (except in the engine model data calculations).

The main assumption is that the gas density number is the only parameter that governs the physical process of the jet generation by the plasma discharge. A process of collisions between ions and neutral molecules create the forces that result in the jet. The collisions are governed by the mean-free-path and the number of molecules in a unit volume. Therefore, with the assumptions listed above, the gas density in laboratory tests should be set to be equal to the density at the application flight conditions.

Assessment of the validity of these assumptions and possible subsequent refinements is a subject of future work. With these assumptions, the main factor affecting the jet generation dependence on pressure and temperature is captured by considering only the density, therefore, the conclusions provide at least a very good approximation.

Validation of the assumption that temperature affects only the density is not trivial. It is known that some of the reactions between different charged molecules and electrons in the plasma are temperature dependent. Usually the dependence is weak except for the temperature dependence of electron attachment processes, which can be significant above 1800 °R (1000 K). It seems that the only practical approach to assess the full effect of temperature and pressure on the momentum transferred to the fluid is to use numerical simulation of the DBD plasma actuator at different temperatures and pressures. This simulation is challenging and is planned to be performed in the future. The authors are not aware of any reported work on this topic.

The assumption that the temperature affects only the density is very reasonable for temperatures under 1800 °R (1000 K). The open question is if it is significant at higher temperature levels. If it turns out that there is divergence from this assumption at all, it is expected to affect the calculated test conditions only for jet engine applications in the combustion chamber and the high-pressure turbine, which are at temperatures higher the 1800 °R, as seen from Figures 4 to 7.

The chamber pressure and temperature to yield the same density as in flight is calculated as follows.

The gas density in the laboratory test chamber should be the same as the density at the application flight conditions,

$$\rho_c = \rho$$

where subscript *c* indicates conditions in the chamber.

Assuming an ideal gas with constant *R*,

$$\rho = P / RT$$

the following relationship is obtained

$$P_c = \frac{P}{\left(T / T_c\right)}$$

where

P_c, T_c, ρ_c – Laboratory chamber pressure, temperature, and density.

P, T, ρ – Static pressure, temperature, and density at flight conditions.

The chamber pressures were calculated first for the case of an air vehicle. Figure 8 shows chamber pressures for simulating flight at altitude for a vehicle with local mach numbers of 0, 0.5, and 1, without shock waves, and for a 20° wedge at M = 2 with a shock wave. The calculations were performed by taking the density at altitude from standard atmosphere data. The atmosphere density is the stagnation density for the air vehicle. Then the isentropic relations were used to calculate the local density at the indicated Mach numbers. For the wedge, shock conditions were used to calculate the density on the wedge surface downstream of shock.

The chamber pressures needed for jet engine applications were calculated from the engine model data for the four generic engine classes. In these calculations sea-level pressure was 17.7 psi. Sea-level temperature was 545.7 °R (29.8 °C). The latter was also taken as the value of the chamber room temperature. The results are displayed in Figure 9. Some notes on the calculations are provided in the next section.

Discussion

For the air vehicle application the chamber pressures decrease with altitude according to the variation of the density with altitude and the local flow conditions at the actuator location. The situation is more complex for the jet engine. The results show that the test chamber pressure varies greatly, from sub-atmospheric to above atmospheric pressures, depending on the operating conditions and location of the placement of the actuator in the engine. For example, if a DBD plasma actuator is to be placed at the inlet to the high pressure turbine for the 300 PAX engine, it has to be tested at 6 atm if it is intended to operate at sea-level takeoff conditions, and at 2.9 atm if it is intended to operate at 35,000 ft cruise. If it is to be used in the exit of high-pressure compressor duct (burner inlet) it has to be tested at 12.4 atm at takeoff conditions, and at 6.2 atm at 35,000 ft cruise conditions. If it is to be used at the low-pressure turbine exit, it has to be tested at 0.5 atm for operation at takeoff, and at 0.2 atm at cruise. If the actuator is to be placed on the low-pressure turbine of the 50 PAX engine flying at 65,000 ft, its performance has to be tested at a very low chamber pressure of 0.03 atm.

Note that the calculations are based on conditions at the inflow and outflow planes of the various engine components. The calculated points are connected with straight lines. Further modification is needed to account for local flow conditions inside the component. For example, in turbomachinery there are inter-row and inter-stage variations, and in inter-blade passages there is acceleration or diffusion or even shock waves that will modify the results. Those local modifications are not included in this study and are left for future work.

Note also that the results shown in Figure 9 display the chamber pressures based on total (stagnation) as well as static conditions in the engine. The reason that the results corresponding to total condition are shown is that the total conditions are equal to static condition at locations where the velocity is zero, corresponding to placement of the actuator at locations such as the leading edge of a turbine or compressor airfoil. As can be seen in the figure, the differences are not large.

Additional insights can be gained from the distribution of the unit Reynolds number. Usually low unit Reynolds number may indicate flow separation. For example, it is known that there is a flow separation problem on the low pressure turbine (LPT) at altitude. Those locations are good candidates for implementation of active flow control. However, those locations are also characterized by low density, requiring the plasma actuator to be tested at low chamber pressures. DBD plasma actuators may suffer from loss of performance as the pressure is decreased (note that there are insufficient and conflicting results in published literature). Therefore, laboratory testing is critical to establish that the DBD actuators can perform adequately under those conditions.

It is important to note that in the field of weakly ionized plasma research, laboratory experiments were traditionally performed in a vacuum chamber at room temperature. It therefore became common in that field to specify the chamber pressure as an experimental parameter. This may have led to habitually considering the pressure, rather than the density, as the relevant parameter.

Conclusions

Data on flow conditions in four generic jet engines, representing four different thrust classes, was presented, and because it is non-proprietary, the data is useful for various applications related to formulating test conditions of flow control devices placed in various engine components. The data was used to develop test conditions for characterization of DBD plasma actuators in a chamber at room temperature. The underlying assumption is that the performance of DBD actuators depends only on the density and that all other temperature-related effects are negligible at the temperature range existing in the jet engine. Based on this assumption and the engine models data, the pressure needed to be set in the test chamber to simulate in-flight engine operating conditions was calculated. The pressures vary with the location of the actuator in the engine, the type of engine, and the flight operating conditions. There is a wide spread in the pressure range, depending on the specific application. The pressure varies from 12.4 to 0.03 atm for the four engine models and flight conditions studied. Chamber pressures needed to test actuators for flight vehicle were also shown. Unlike the engine environment, the flow conditions for testing flight vehicles can simply be calculated with data readily available from standard atmospheric tables, for any flight speed and altitude.

References

1. Lord, W.K., MacMartin, D.G., and Tillman G., “Flow Control Opportunities in Gas Turbine Engines,” AIAA–2000–2234, 2000.
2. Likhanskii, A.V., Shneider, M.N., Macheret, M.O., and Miles, R.B., “Modeling of Interaction Between Weakly Ionized Near-Surface Plasmas and Gas Flow,” AIAA–2006–1204, 2006.
3. Likhanskii, A.V., Shneider, M.N., Opaits, D.F., Miles, R.B., and Macheret, S.O., “Numerical Modeling of DBD Plasma Actuators and the Induced Air Flow,” AIAA–2007–4533, 2007.
4. Likhanskii, A.V., “Study of Plasma Phenomena at High Electric Fields in Applications for Active Flow Control and Ultra-Short Pulse Laser Drilling,” Ph.D. Dissertation, The Pennsylvania State University, College Station, PA, 2009.
5. Corke, T.C., Jumper, E.J., Post, M.L., Orlov, D., and McLaughlin, T.E., “Application of Weakly-Ionized Plasmas as Wing Flow-Control Devices,” AIAA–2002–350, 2002.
6. Suzen, Y.B., Huang, P.G., Jacob, J.D., and Ashpis, D.E., “Numerical Simulations of Plasma Based Flow Control Applications,” AIAA–2005–4633, 2005.
7. Suzen, Y.B., Huang, P.G., and Ashpis, D.E., “Numerical Simulations of Flow Separation Control in Low-Pressure Turbines Using Plasma Actuators,” AIAA–2007–937, 2007.
8. Samimy, M., Adamovich, I., Webb, B., Kastner, J., Hileman, J., Keshav, S., and Palm, P., “Development and Characterization of Plasma Actuators for High Speed and Reynolds Number Jet Control,” Experiments in Fluids, Vol. 37 (4), 2004, pp. 577–588.
9. Moreau, E., “Airflow Control by Non-Thermal Plasma actuators,” J. Phys. D: Appl. Phys. Vol. 40, 2007, pp. 605–636.
10. Corke, T.C., Post, M.L., and Orlov, D.M., “SDBD Plasma enhanced Aerodynamics: Concepts, Optimization and Applications,” Progress in Aerospace Sciences Vol. 43, 2007, pp. 193–217.
11. Corke, T.C., Post, M.L., and Orlov, D.M., “Single Dielectric Barrier Discharge Plasma Enhanced Aerodynamics: Physics, Modeling and Applications,” Exp. Fluids, Vol. 46, 2009, pp. 1–26.
12. Corke, T.C., Enloe, C.L., and Wilkinson, S.P., “Dielectric Barrier Discharge Plasma Actuators for Flow Control,” Annu. Rev. Fluid Mech. Vol. 42, 2010, pp. 505–29.
13. Hultgren, L.S., and Ashpis, D.E., “Demonstration of Separation Delay with Glow-Discharge Plasma Actuators,” AIAA–2003–1025, 2003.
14. List, J., Byerley, A.R., McLaughlin, T.E., and VanDyken, R.D., “Using a Plasma Actuator to Control Laminar Separation on a Linear Cascade Turbine Blade,” AIAA–2003–1026, 2003.
15. Huang J., Corke T.C., and Thomas F.O., “Plasma Actuators for Separation Control of Low Pressure Turbine Blades,” AIAA J., Vol. 44, 2006, pp. 51–57.
16. Huang J., Corke T.C., and Thomas F.O., “Unsteady Plasma Actuators for Separation Control of Low-Pressure Turbine Blades,” AIAA J., Vol. 44, 2006, pp. 1477–87.
17. Morris, S.C., Corke, T.C., VanNess, D., Stephens, J., and Douvillev, T., “Tip Clearance Control Using Plasma Actuators,” AIAA–2005–782, 2005.
18. VanNess, D.K., Corke, T.C., and Morris S.C., “Turbine Tip Clearance Flow Control Using Plasma Actuators,” AIAA–2006–21, 2006.

19. Douville, T., Stephens J., Corke T., Morris S., “Turbine Blade Tip Leakage Flow Control by Partial Squealer Tip and Plasma Actuators,” AIAA–2006–20, 2006.
20. VanNess, D.K., Corke, T.C., and Morris S.C., “Tip Clearance Flow Visualization of a Turbine Blade Cascade with Active and Passive Flow Control,” ASME Paper No. GT2008-5070, 2008.
21. Göksel, B., Fischer, M., Rechenberg, I., and Thallemer, A., “Elektrostatischer Plasma-Wellantrieb für Bionische Luftschiffe,” Proceedings of the German Aerospace Congress 2005, Friedrichshafen, Germany, Deutsche Gesellschaft für Luft- und Raumfahrt Paper No. DGLR-2005-261, Vol. 3, 2005, pp. 1853–1856.
22. Göksel, B., Private Communication, 2008, http://www.electrofluidsystems.com/airfish/b-ionic-airfish-2008.wmv
23. Sidorenko, A., Budovsky, A., Pushkarev, A., and Maslov, A., “Flight Testing of DBD Plasma Separation Control System,” AIAA–2008–373, 2008.
24. Grundmann, S., Frey, M., and Tropea, C., “Unmanned Aerial Vehicle (UAV) with Plasma Actuators for Separation Control,” AIAA–2009–698, 2009.
25. Abe, T., Takizawa, Y., Sato, S., and Kimura, N., “A Parametric Experimental Study for Momentum Transfer by Plasma Actuator,” AIAA–2007–187, 2007.
26. Gregory, J.W., Enloe, C.L., Font, G.I., and McLaughlin, T., “Force Production Mechanisms of a Dielectric-Barrier Discharge Plasma Actuator,” AIAA–2007–185, 2007.
27. Schuele, C.Y. and Corke, T., “Characteristics of Single Dielectric Barrier Discharge Plasma Actuators at Sub-atmospheric Pressures,” 61st Annual Meeting of the APS/DFD, San Antonio, Texas, Nov. 2008, http://meetings.aps.org/link/BAPS.2008.DFD.ET.9
28. Takagaki, M., Isono, S., Nagai, H., and Asai, K., “Evaluation of Plasma Actuator Performance in Martian Atmosphere for Applications to Mars airplanes,” AIAA–2008–3762, 2008.
29. Benard, N., Balcon, N., and Moreau, E., “Electric Wind Produced by a Surface Dielectric Barrier Discharge Operating in Air at Different Pressures: Aeronautical Control Insights,” J. Phys D: Appl. Phys., Vol. 41, 2008, pp. 042002.
30. Benard, N., Balcon, N., and Moreau, E., “Electric Wind Produced by a Single Dielectric Barrier Discharge Actuator Operating in Atmospheric Flight Conditions: Pressure Outcome,” AIAA–2008–3792, 2008.
31. Valerioti, J., and Corke, T., “Effect of Dielectric Properties on Functional Relationship between Plasma Initiation and Ambient Pressure,” 62nd Annual Meeting of the APS/DFD, Minneapolis, MN, Nov 2009. http://meetings.aps.org/link/BAPS.2009.DFD.GD.1
32. Font, G.I., Enloe, C.L., Newcomb, J.Y., Teague, A.L., Vasso, A.R., and McLaughlin, T.E., “Effects of Oxygen Content on the Behavior of the Dielectric Barrier Discharge Aerodynamic Plasma Actuator,” AIAA–2010–545, 2010.
33. Benard, N., and Moreau, E., “Effects of Altitude on the Electromechanical Characteristics of Dielectric Barrier Discharge Plasma Actuators,” AIAA–2010–4633, 2010.
34. Valerioti, J.A., “Pressure Dependence of Plasma Actuated Flow Control,” MS Thesis, University of Notre Dame, Indiana, 2010.
35. Valerioti, J., and Corke, T., “Pressure Dependence of Plasma Actuated Flow Control,” 63rd Annual Meeting of the APS Division of Fluid Dynamics, Long Beach, California, November 2010. http://meetings.aps.org/link/BAPS.2010.DFD.QJ.4
Also: Submitted for AIAA Journal.
36. Lytle, J.K., “The Numerical Propulsion Simulation: An Overview,” NASA/TM—2000-209915, 2000.
37. Jones, S.M., “An Introduction to Thermodynamic Performance Analysis of Aircraft Gas Turbine Engine Cycles Using the Numerical Propulsion System Simulation Code,” NASA/TM—2007-214690, 2007.
38. Tong, M.T., Naylor, B.A., “An Object-Oriented Computer Code for Aircraft Engine Weight Estimation,” ASME Paper No. GT2008-50062, 2008.

TABLE 1.—PARAMETERS OF FOUR ENGINE MODELS

Engine	Thrust	Weight	OPR		BPR
	At sea-level static	Bare engine	Overall Pressure Ratio		Bypass Ratio
	(lbf)	(lb)	At sea-level	At 35k ft	At 35k ft
300PAX	86,700	18,400	37.8	45.7	8.3
150PAX (future)	23,400	5,100	33.5	42.0	14.3
50PAX	7,600	1,300	23.5	28.4	5.3
Military	18,500	3,800	33.4	33.6	0.4

TABLE 2.—AXIAL COORDINATES OF ENGINE MODEL COMPONENTS

300 PAX		150 PAX		50 PAX		Military	
X, in.	**Component outflow plane**	**X, in.**	**Component outflow plane**	**X, in.**	**Component outflow plane**	**X, in.**	**Component outflow plane**
Core		**Core**		**Core**		**Core**	
–60	Ambient	–45	Ambient	–20	Ambient	–20	Ambient
0	Inlet	0	Inlet	0	Inlet	0	Inlet
24	Fan	15	Fan	6	Fan	22	Fan
24	Splitter	15	Splitter	12	Duct	25	Duct
26	Duct	15	Duct	46	HPC	56	HPC
46	LPC	28	LPC	48	Duct	60	Duct
59	Duct	39	Duct	55	Burner	69	Burner
110	HPC	65	HPC	58	HPT	77	HPT
111	Duct	66	Duct	59	Duct	78	TDuct
120	Burner	73	Burner	71	LPT	86	LPT
129	HPT	77	HPT	86	Mixer	95	Mixer
138	Duct	84	Duct	103	Nozzle	106	Duct
181	LPT	100	LPT	**Bypass**		146	Augmentor
188	Duct	103	Duct	–20	Ambient	190	Nozzle
212	Core Nozzle	115	Core Nozzle	0	Inlet	**Bypass**	
Bypass		**Bypass**		6	Fan	–20	Ambient
–60	Ambient	–45	Ambient	71	Duct	0	Inlet
0	Inlet	0	Inlet	86	Duct	22	Fan
24	Fan	15	Fan			86	Duct
24	Splitter	15	Splitter			95	Mixer
59	Bypass EGV	30	Bypass EGV				
95	Duct	47	Duct				
149	Bypass Nozzle	86	Bypass Nozzle				

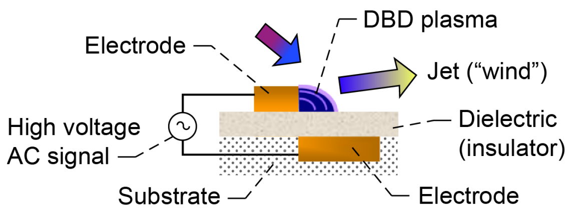

Figure 1.—Schematic of a DBD plasma actuator.

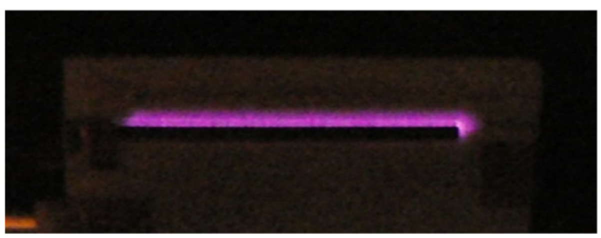
Figure 2.—Top view of typical DBD discharge (Alumina dielectric with copper electrodes, NASA GRC experiment).

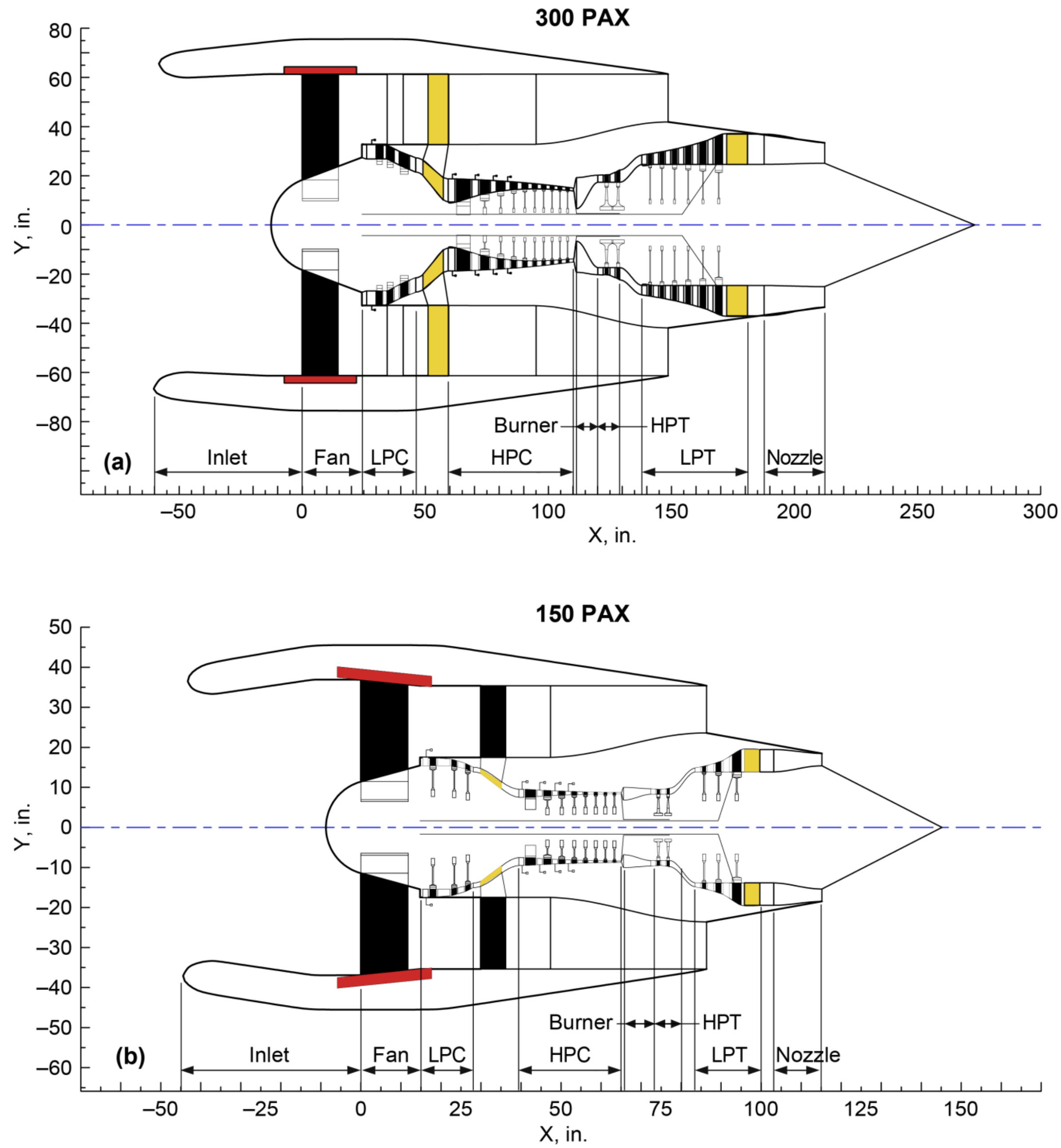

Figure 3.—Schematics of four engine models. (a) 300 PAX. (b) 150 PAX.

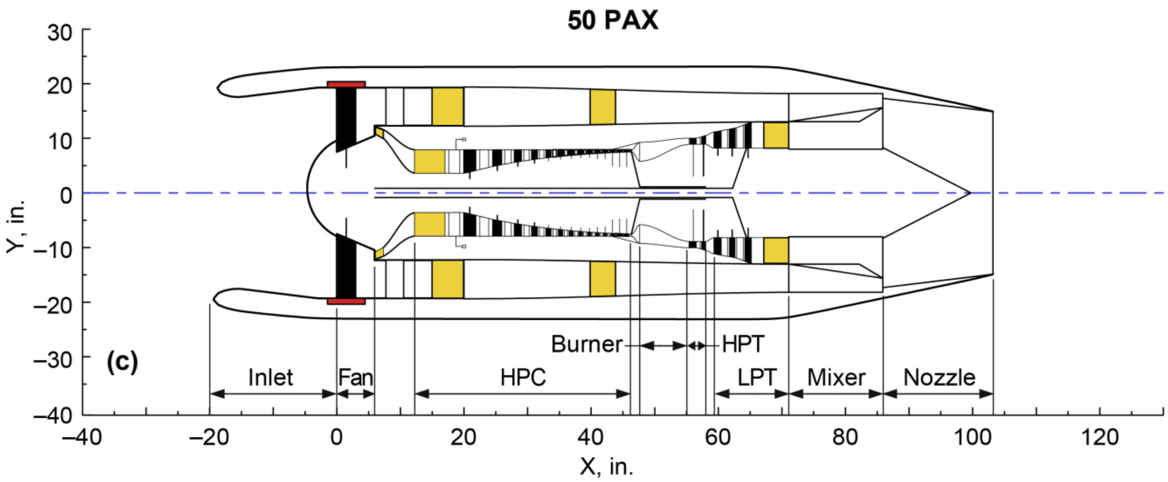

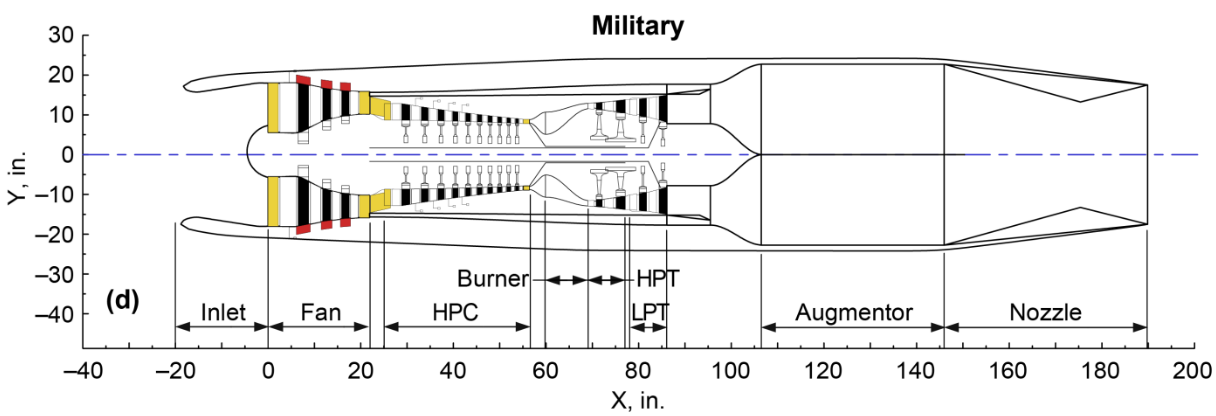

Figure 3.—Schematics (concluded). (c) 50 PAX. (d) Military.

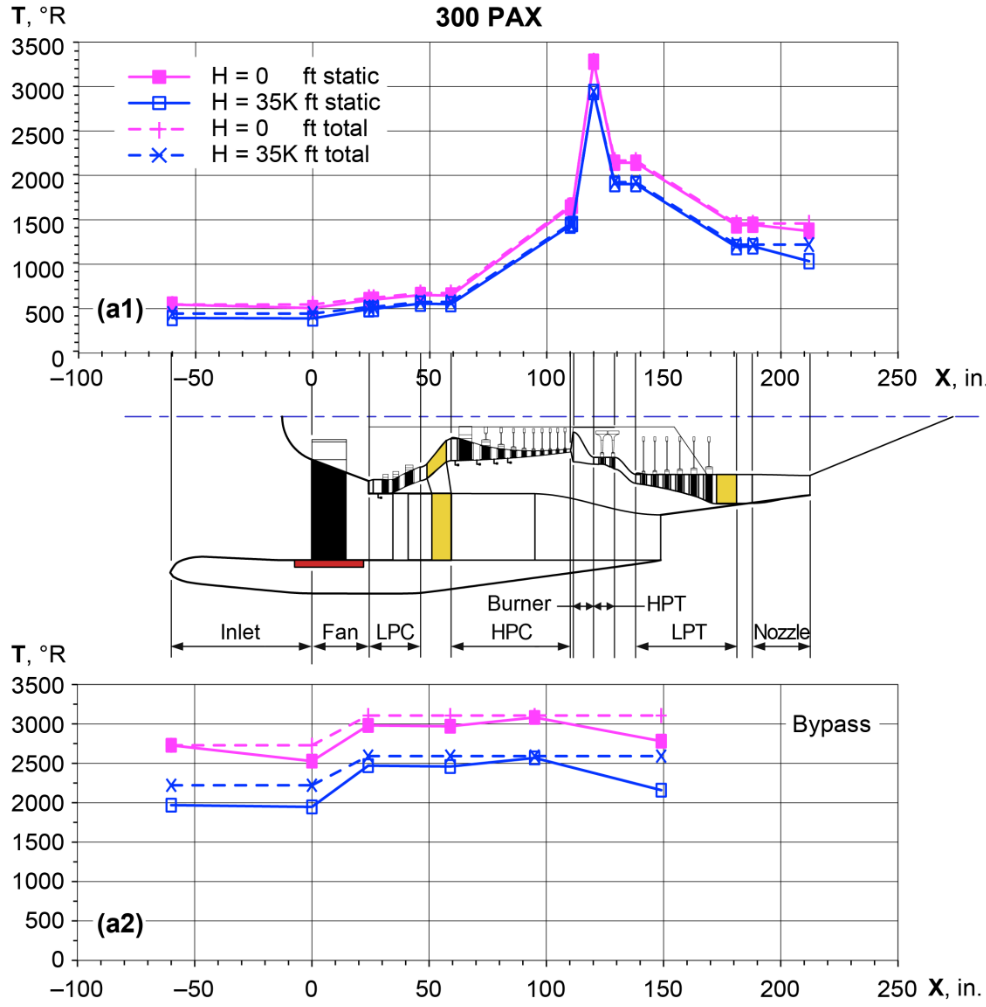

Figure 4a.—300 PAX engine–static and total temperatures. (a1) Core flow-path. (a2) Bypass.

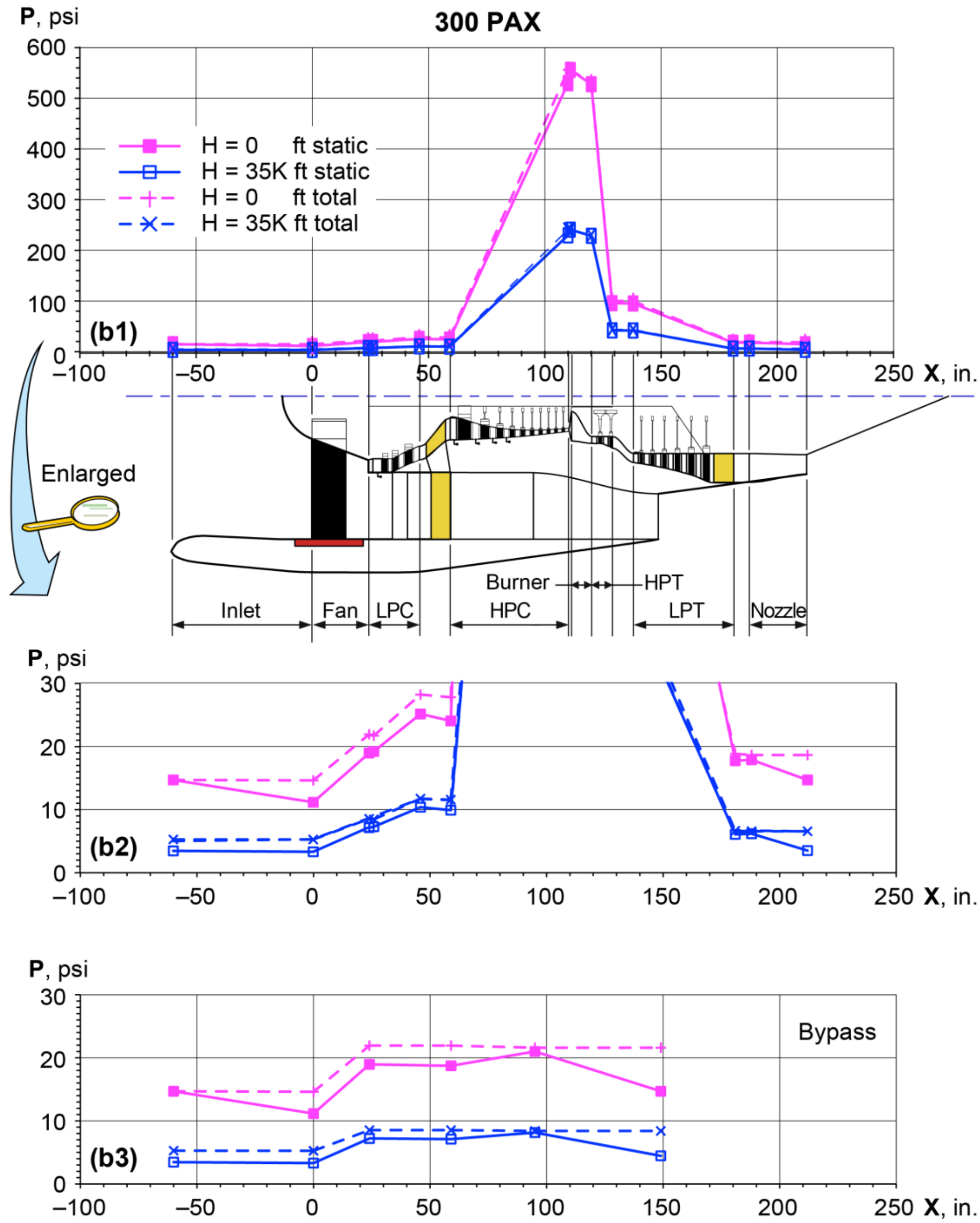

Figure 4b.—300 PAX engine–static and total pressures. (b1) Core flow-path full-pressure scale. (b2) Enlargement of (b1). (b3) Bypass.

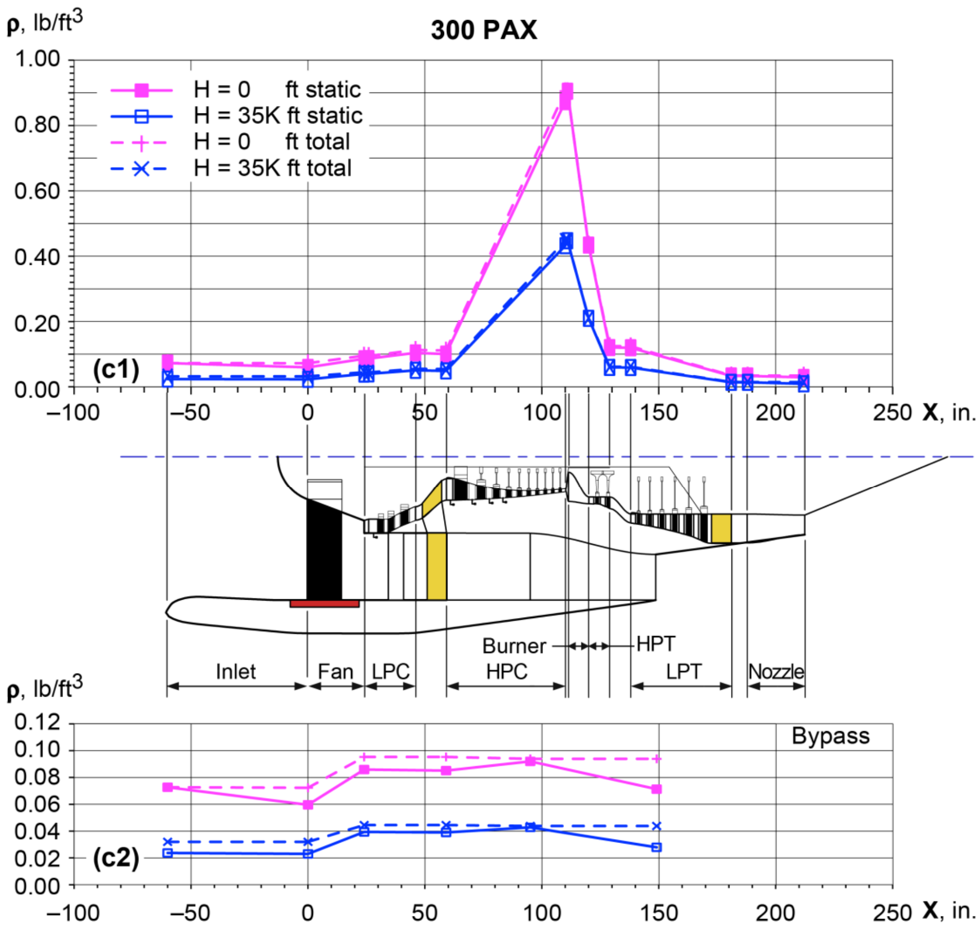

Figure 4c.—300 PAX engine–static and total densities. (c1) Core flow-path. (c2) Bypass.

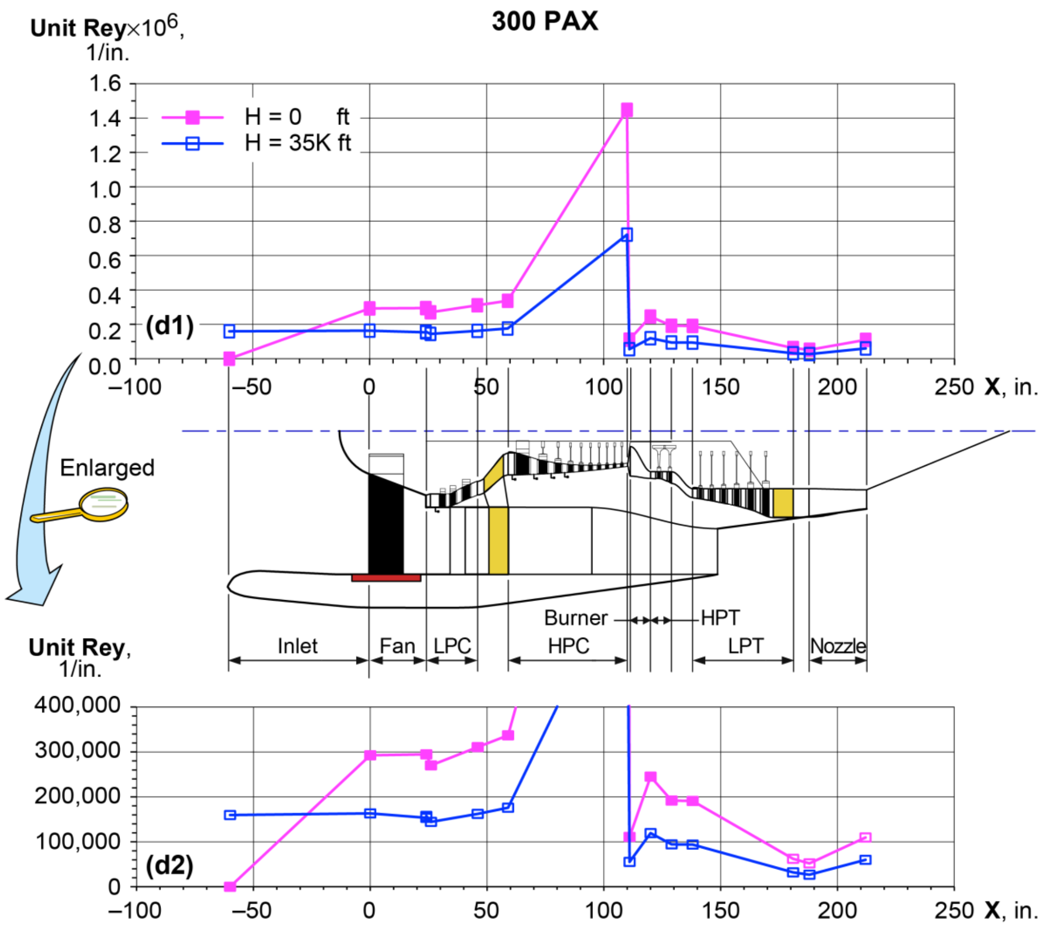

Figure 4d.—300 PAX (d1) unit Reynolds number in core flow-path. Full unit Reynolds number scale. (d2) Enlargement.

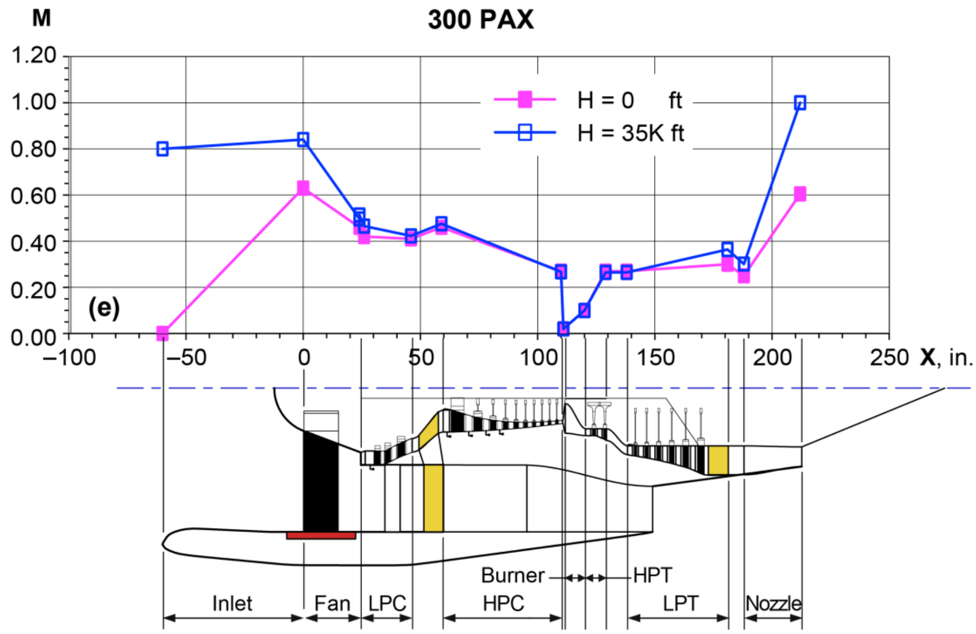

Figure 4e.—300 PAX engine–Mach number in the core flow-path.

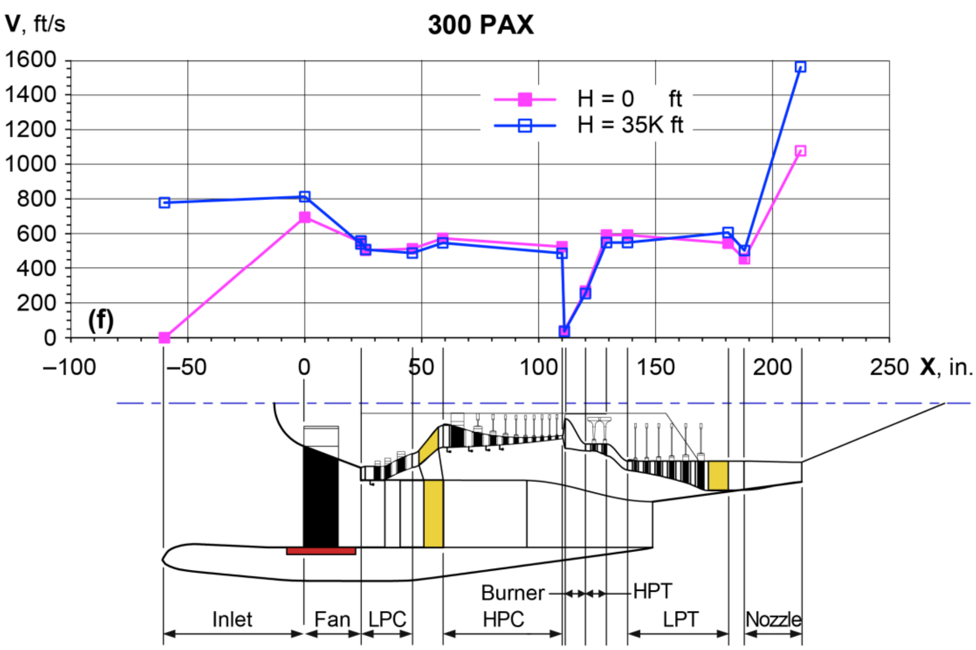

Figure 4f.—300 PAX engine–Velocity in the core flow-path.

Figure 4.—Engine data for 300 PAX engine model (a) Temperatures. (b) Pressures. (c) Density. (d) Unit Reynolds number. (e) Mach number, (f) Velocity, for sea-level takeoff and 35,000 ft cruise.

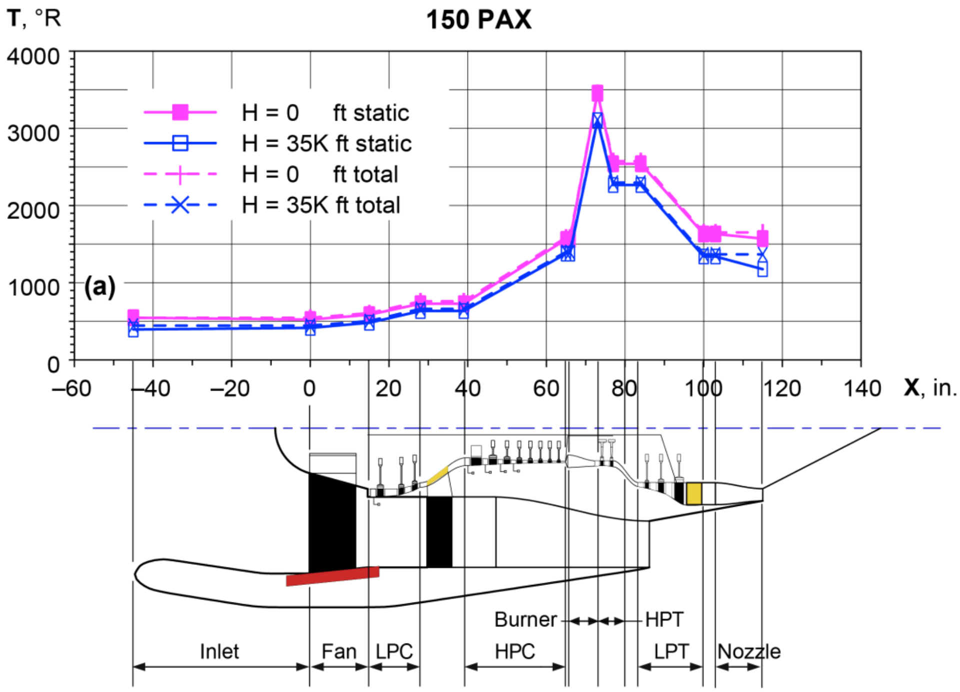

Figure 5a.—150 PAX engine–static and total temperatures.

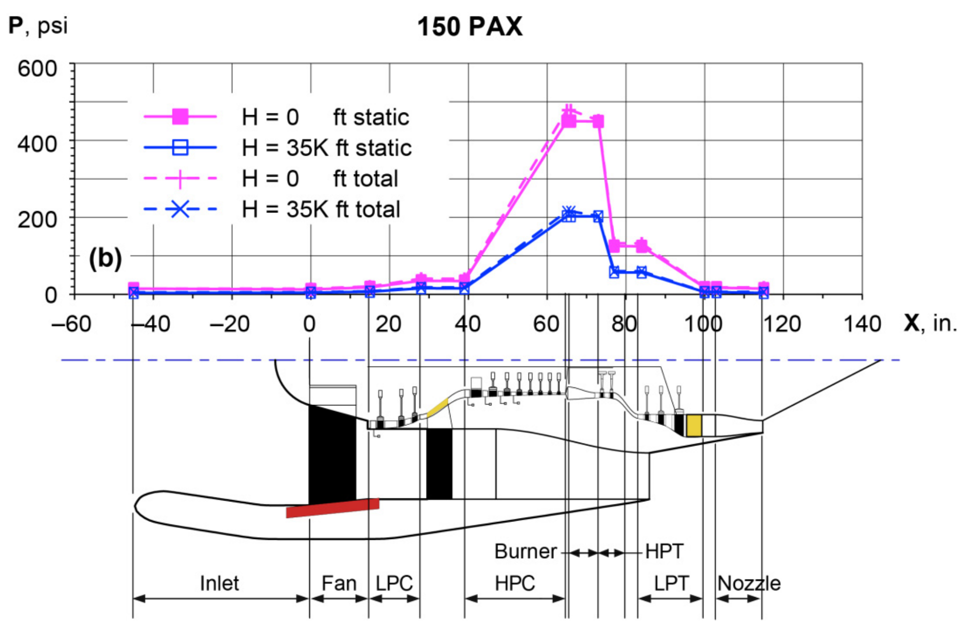

Figure 5b.—150 PAX engine–static and total pressures.

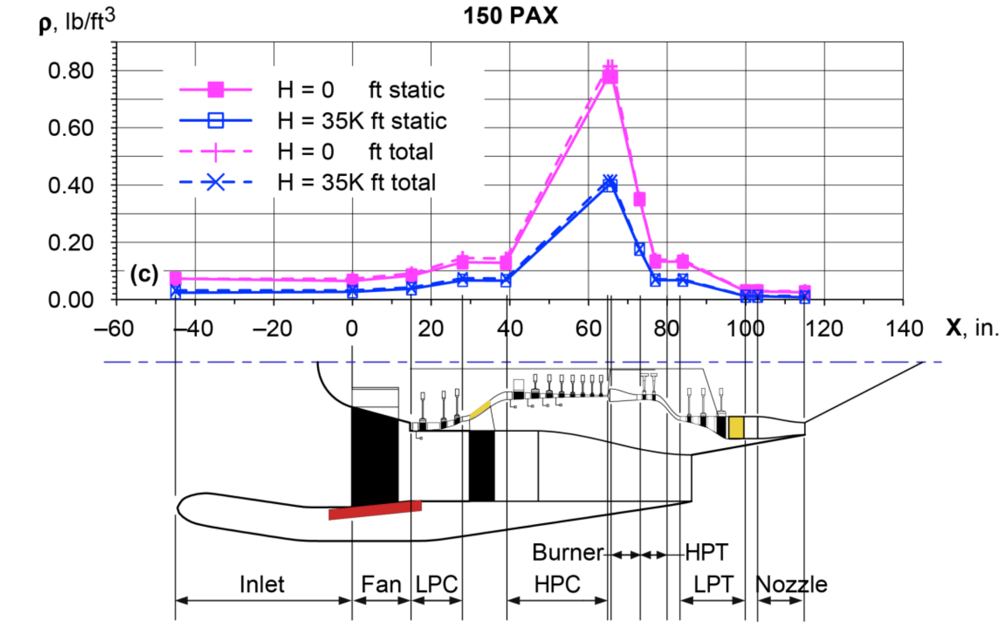

Figure 5c.—150 PAX engine–static and total densities.

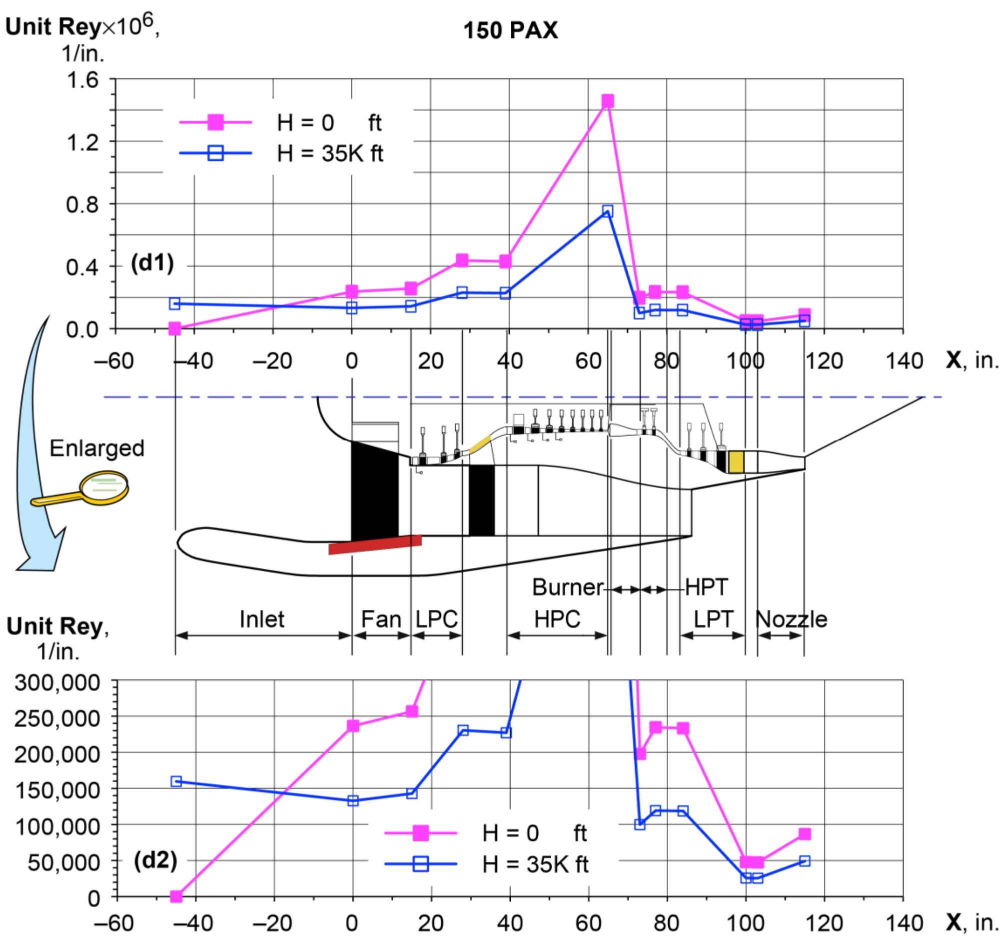

Figure 5d.—150 PAX engine–unit Reynolds numbers. (d1) Full unit Reynolds number scale. (d2) Enlargement.

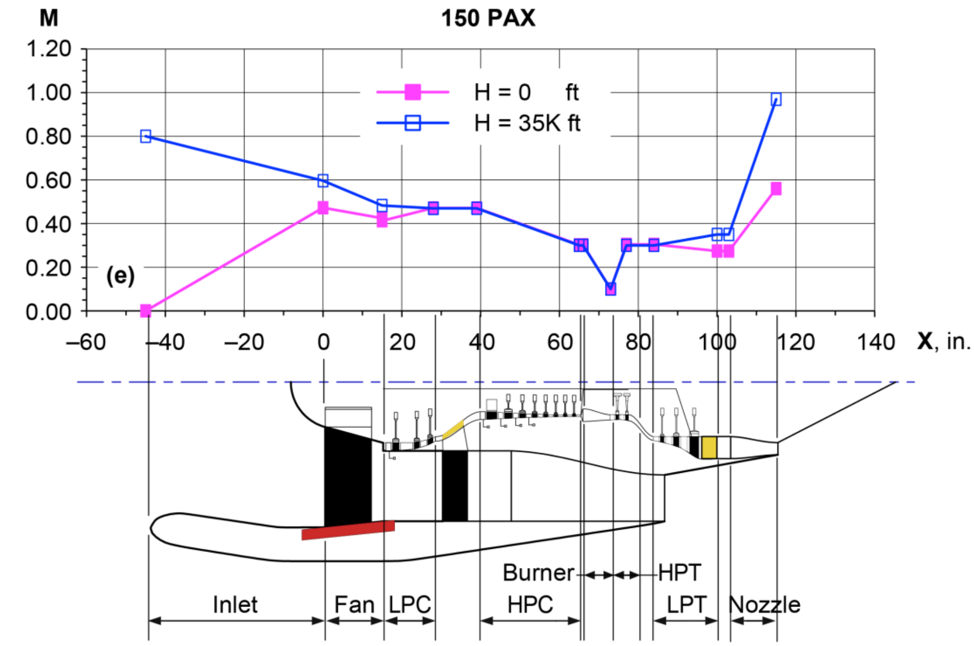

Figure 5e. 150 PAX engine–Mach number.

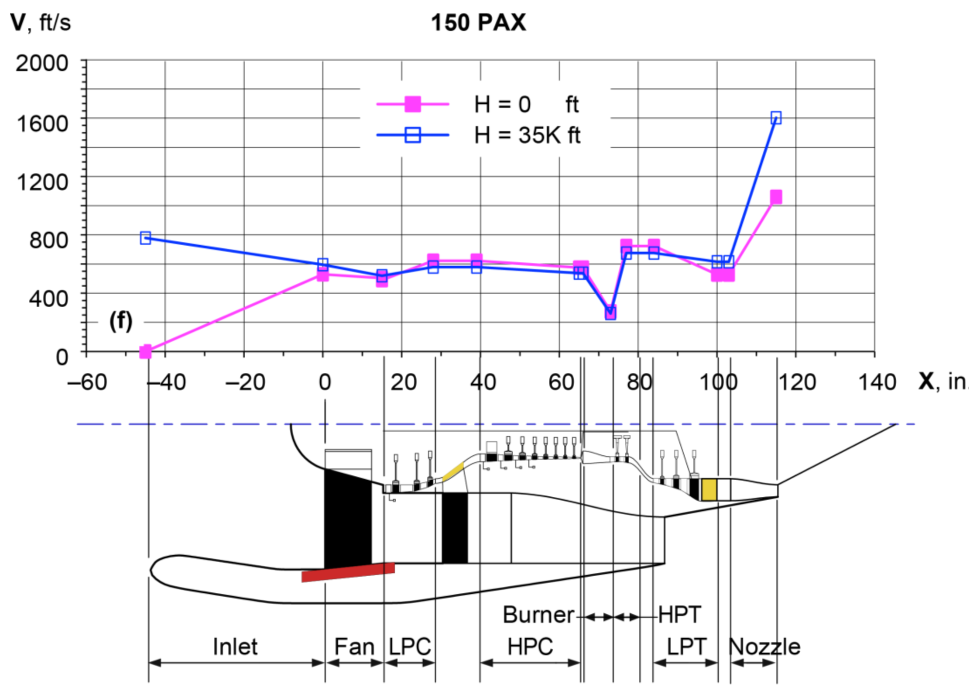

Figure 5f. 300 PAX engine–Velocity.

Figure 5.—Engine data for 150 PAX engine model (a) Temperatures. (b) Pressures. (c) Densities. (d) Unit Reynolds number. (e) Mach number. (f) Velocity, for sea-level takeoff and 35,000 ft cruise.

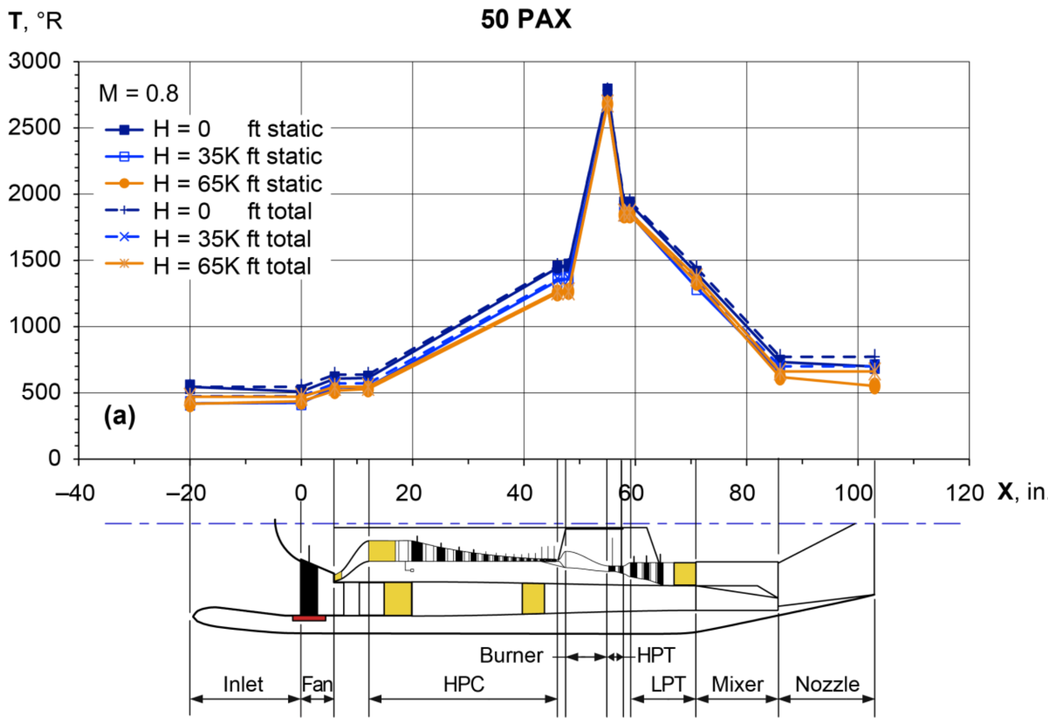

Figure 6a.—50 PAX engine–static and total temperatures, M = 0 at sea level, M = 0.8 at 35,000 ft and 65,000 ft.

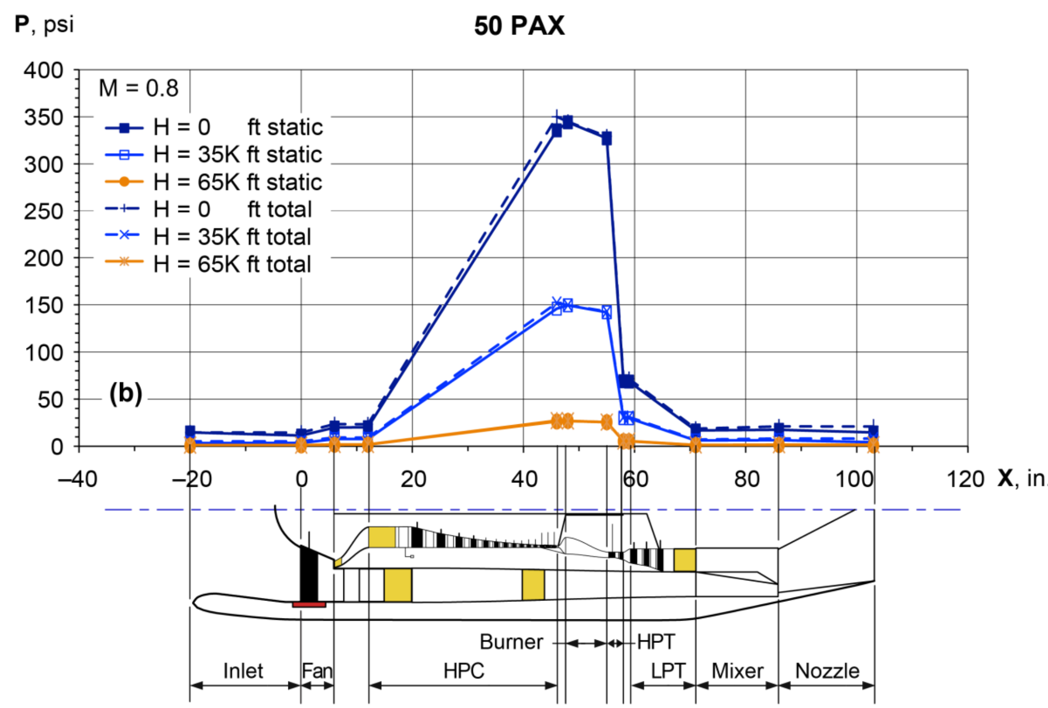

Figure 6b.—50 PAX engine–static and total pressures, M = 0 at sea level, M = 0.8 at 35,000 ft and 65,000 ft.

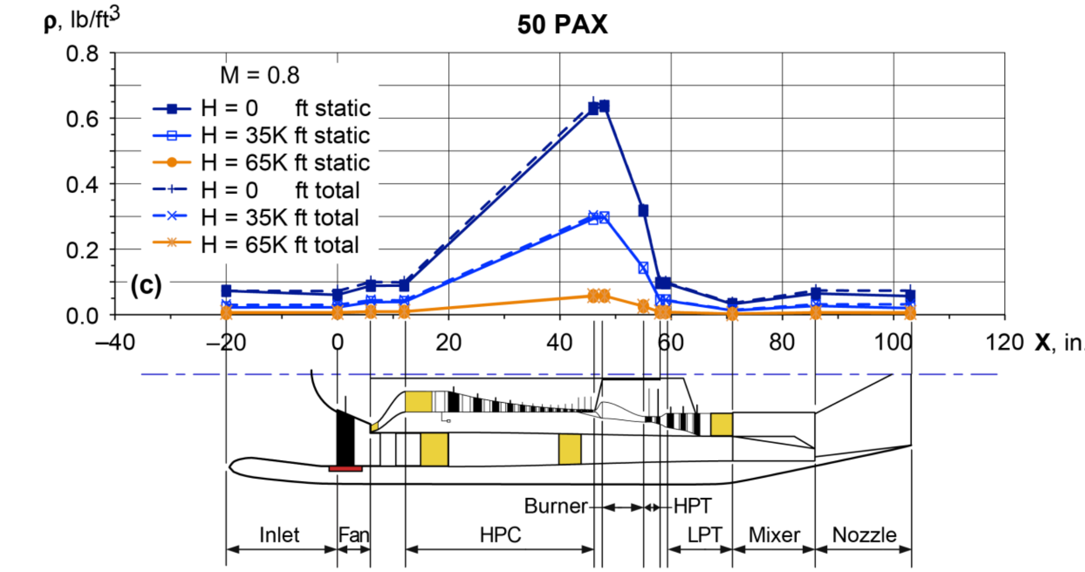

Figure 6c.—50 PAX engine–static and total densities, M = 0 at sea level, M = 0.8 at 35,000 ft and 65,000 ft.

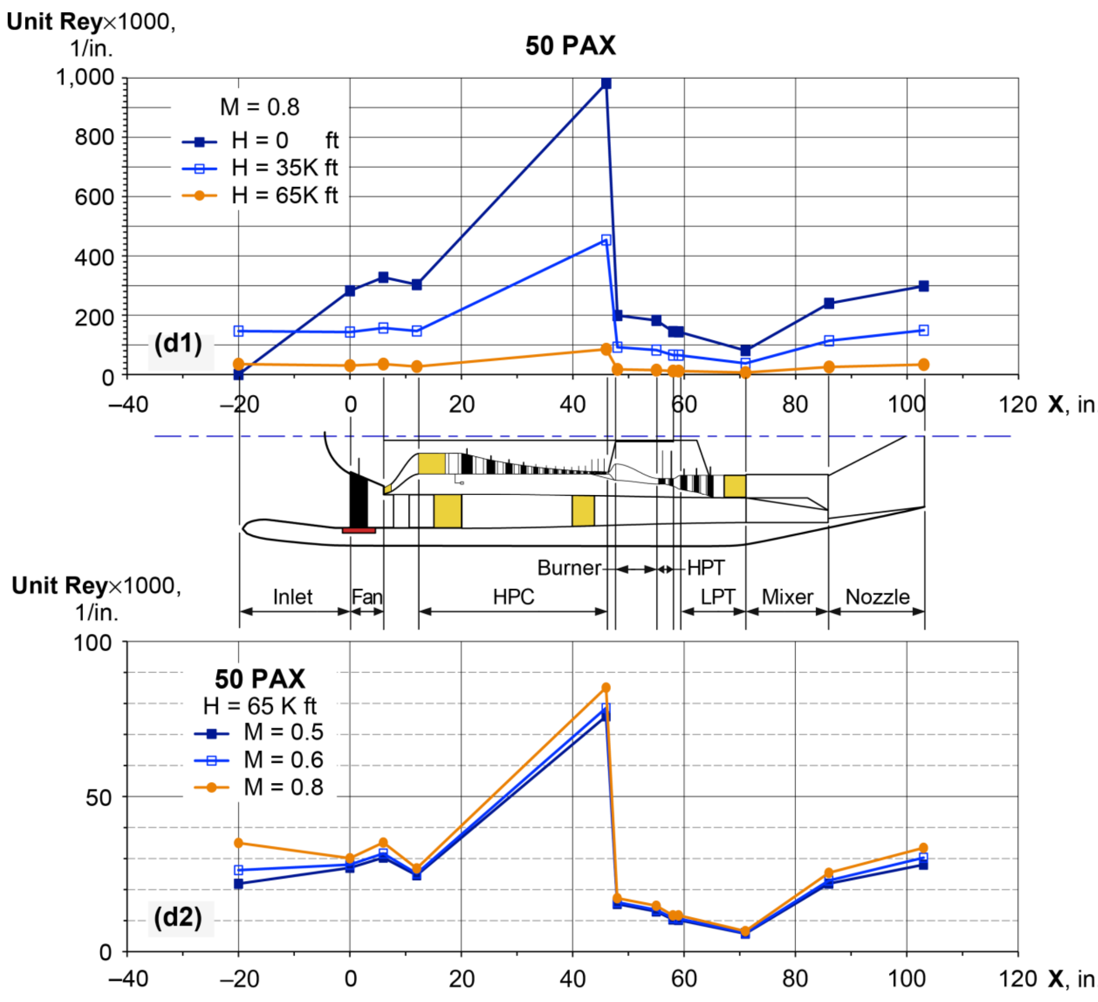

Figure 6d.—50 PAX engine–unit Reynolds number. (d1) For M = 0 at sea level, M = 0.8 at 35,000 ft and 65,000 ft. (d2) For M = 0.5, 0.6, and 0.8 at 65,000 ft.

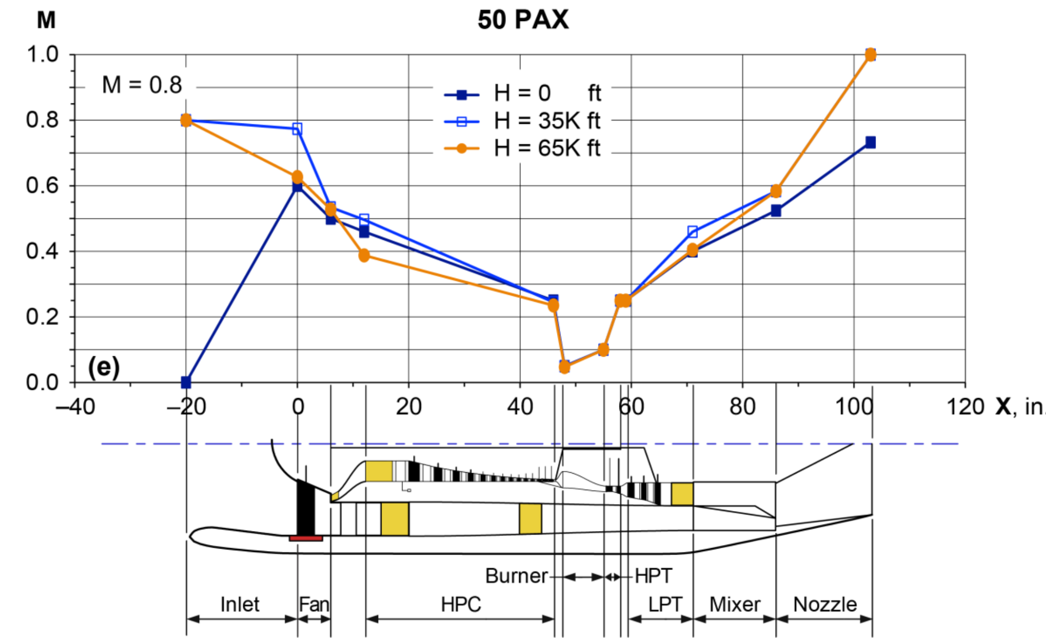

Figure 6e.—50 PAX engine–Mach number, M = 0 at sea level, M = 0.8 at 35,000 ft and 65,000 ft.

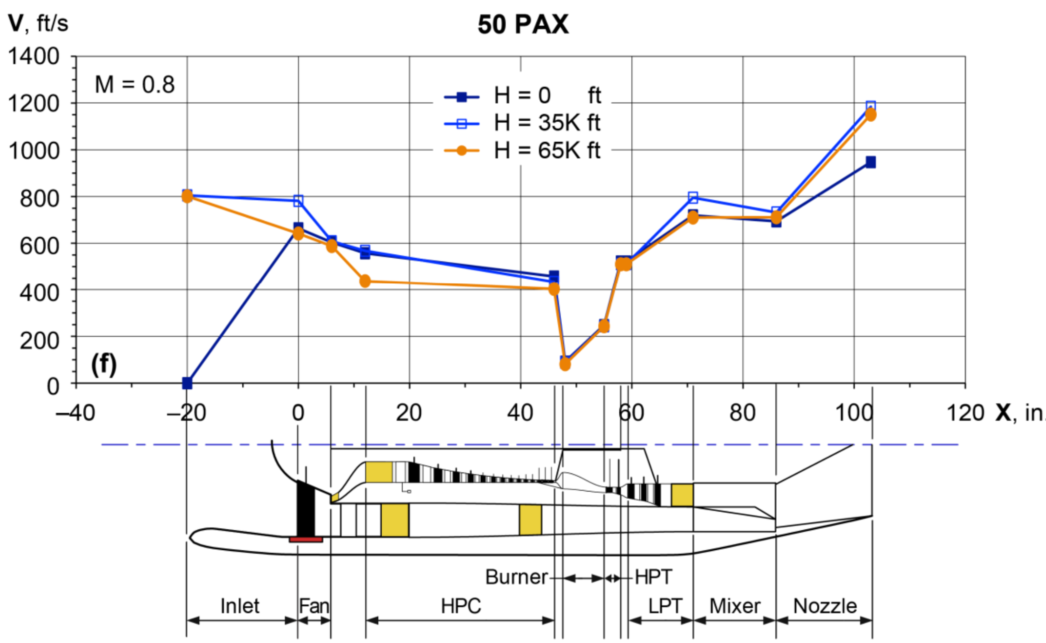

Figure 6f.—50 PAX engine–Velocity, M = 0 at sea level, M = 0.8 at 35,000 ft and 65,000 ft.

Figure 6.—Engine data for 50 PAX engine model (a) Temperatures. (b) Pressures. (c) Densities. (d) Unit Reynolds number. (e) Mach number. (f) Velocity, for sea-level takeoff and 35,000 ft and 65,000 ft cruise.

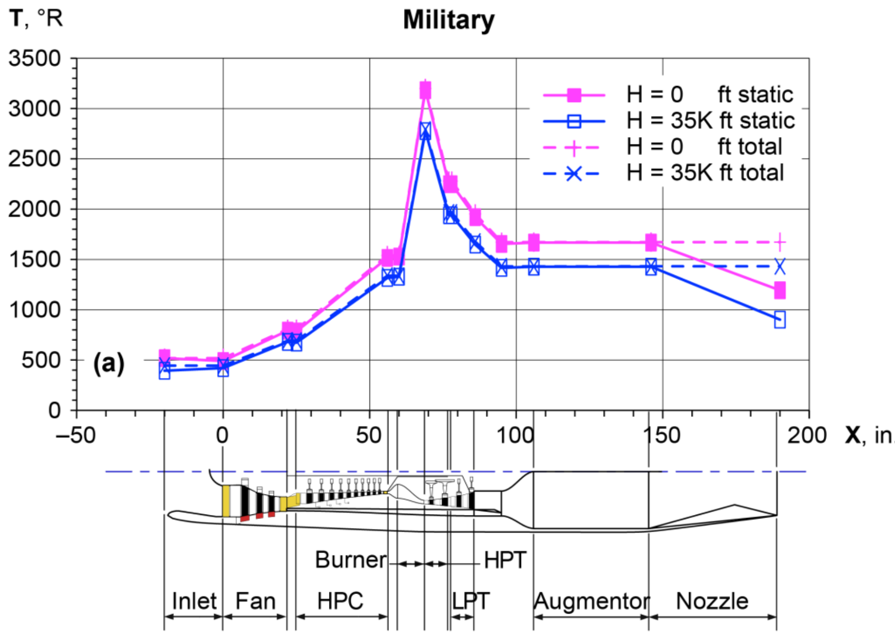

Figure 7a.—Military jet fighter engine–static and total temperatures.

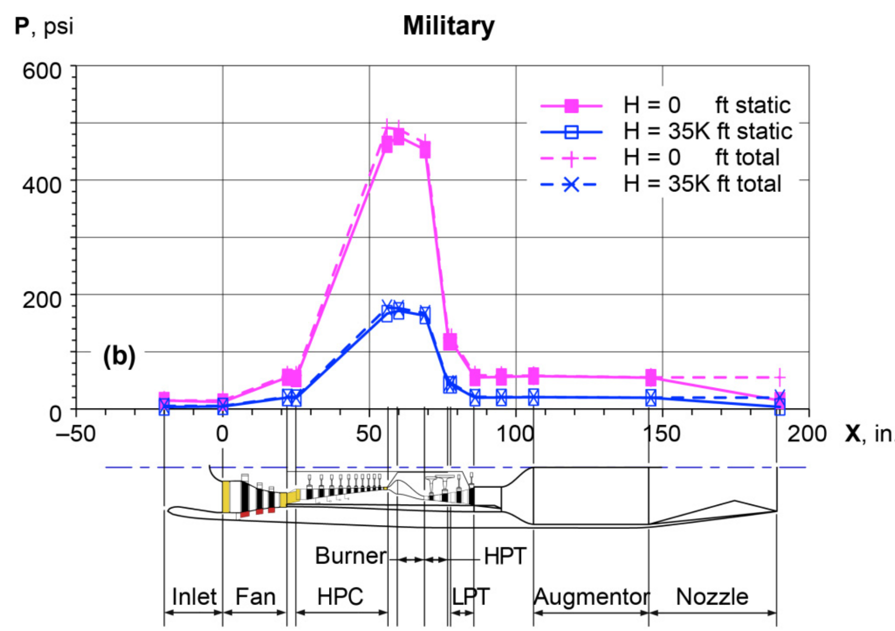

Figure 7b.—Military jet fighter engine–static and total pressures.

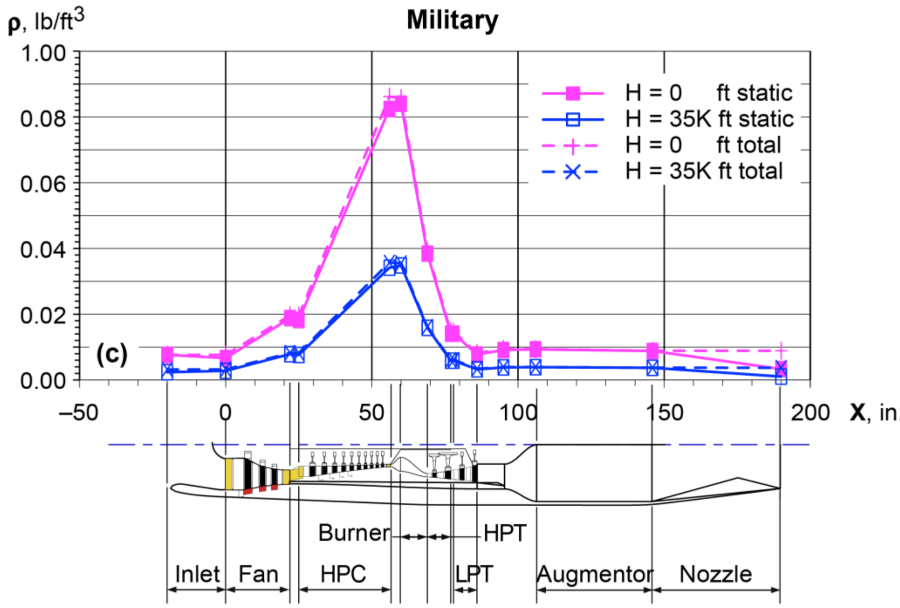

Figure 7c.—Military jet fighter engine–static and total densities.

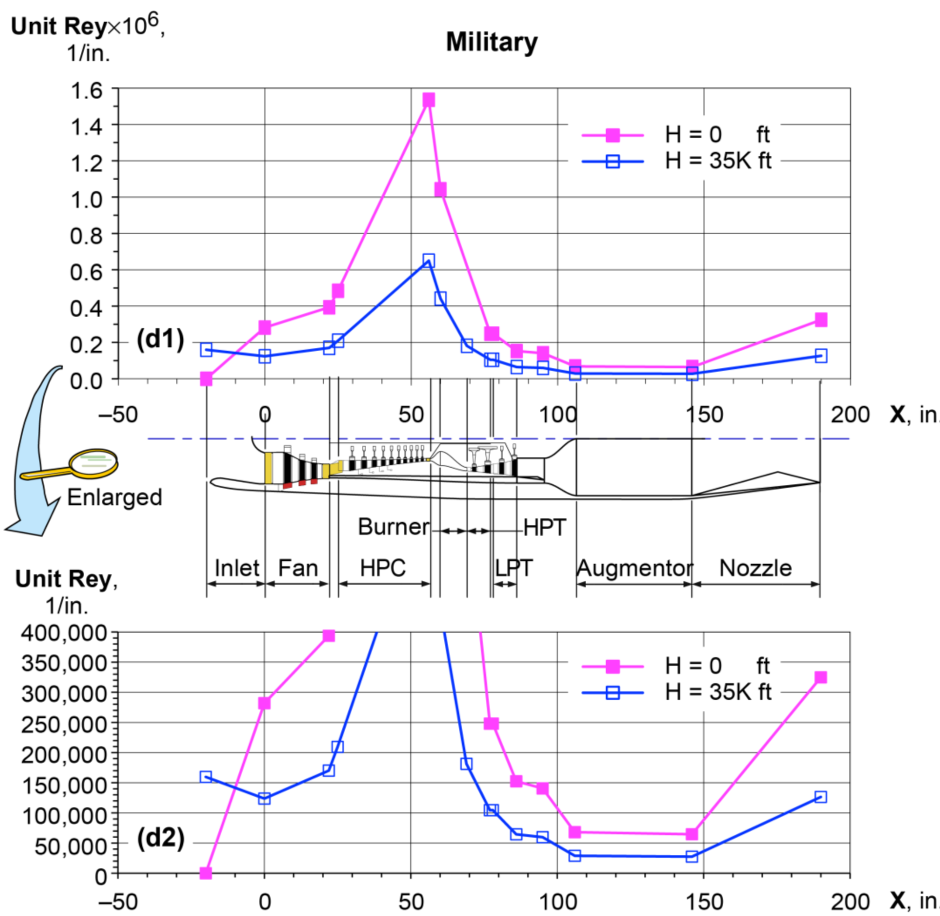

Figure 7d.—Military jet fighter engine–unit Reynolds number. (d1) Full unit Reynolds number scale. (d2) Enlargement.

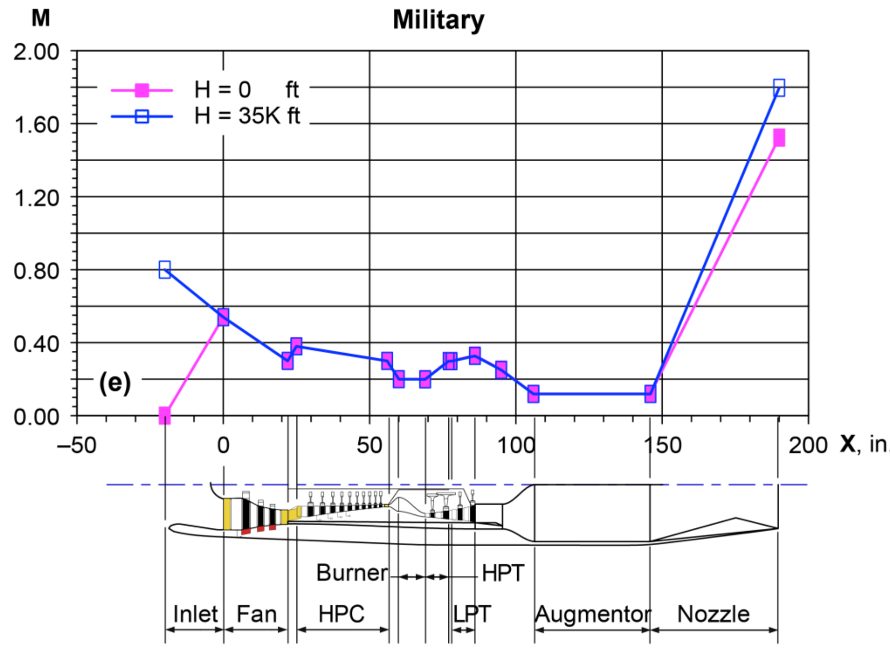

Figure 7e.—Military jet fighter engine–Mach number.

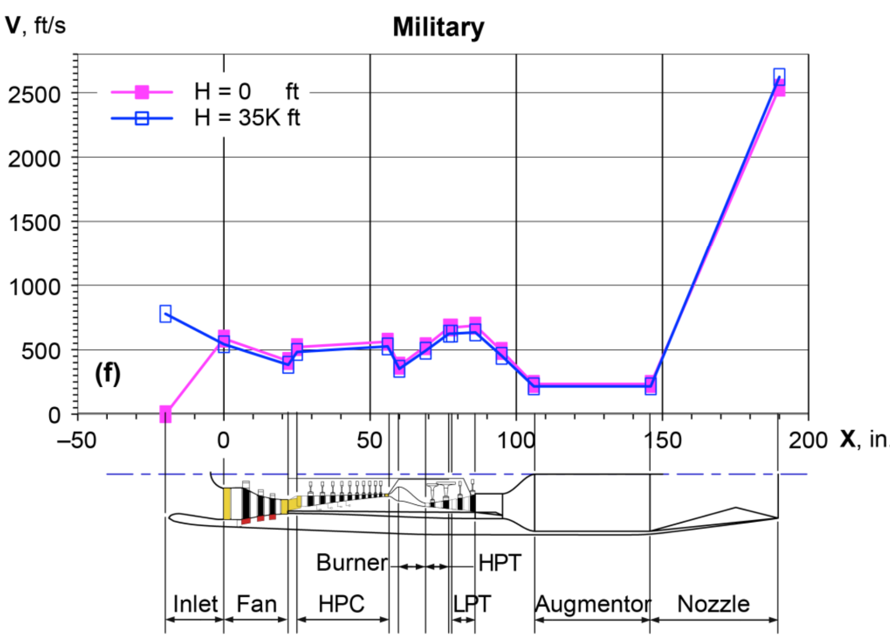

Figure 7f.—Military jet fighter engine–Velocity.

Figure 7.—Military jet fighter engine model (a) Temperatures. (b) Pressures. (c) Densities. (d) Unit Reynolds number. (e) Mach number. (f) Velocity, for sea-level takeoff and 35,000 ft cruise.

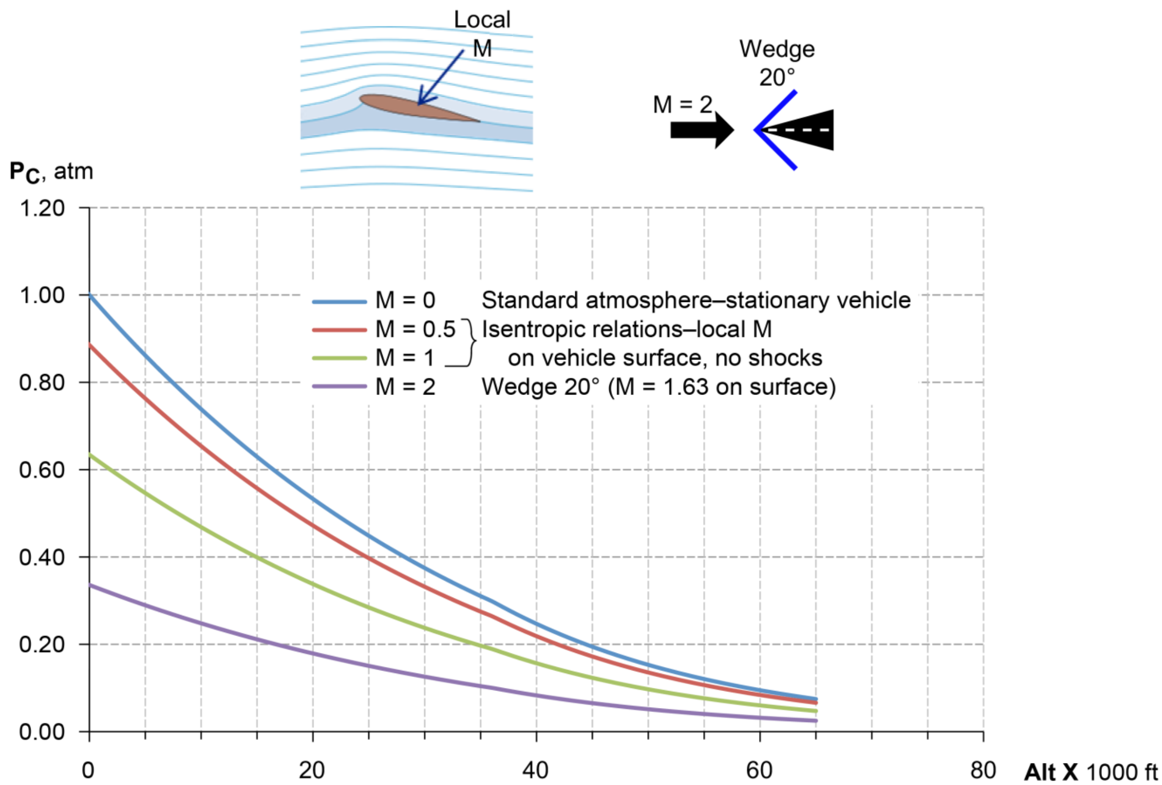

Figure 8.—Chamber pressures for application in air vehicle in altitude flight. The figure shows the chamber pressure needed to match density on the body at local Mach number M = 0, 0.5, and 1 for flow without shock wave, and M = 2 for a wedge with a shock wave.

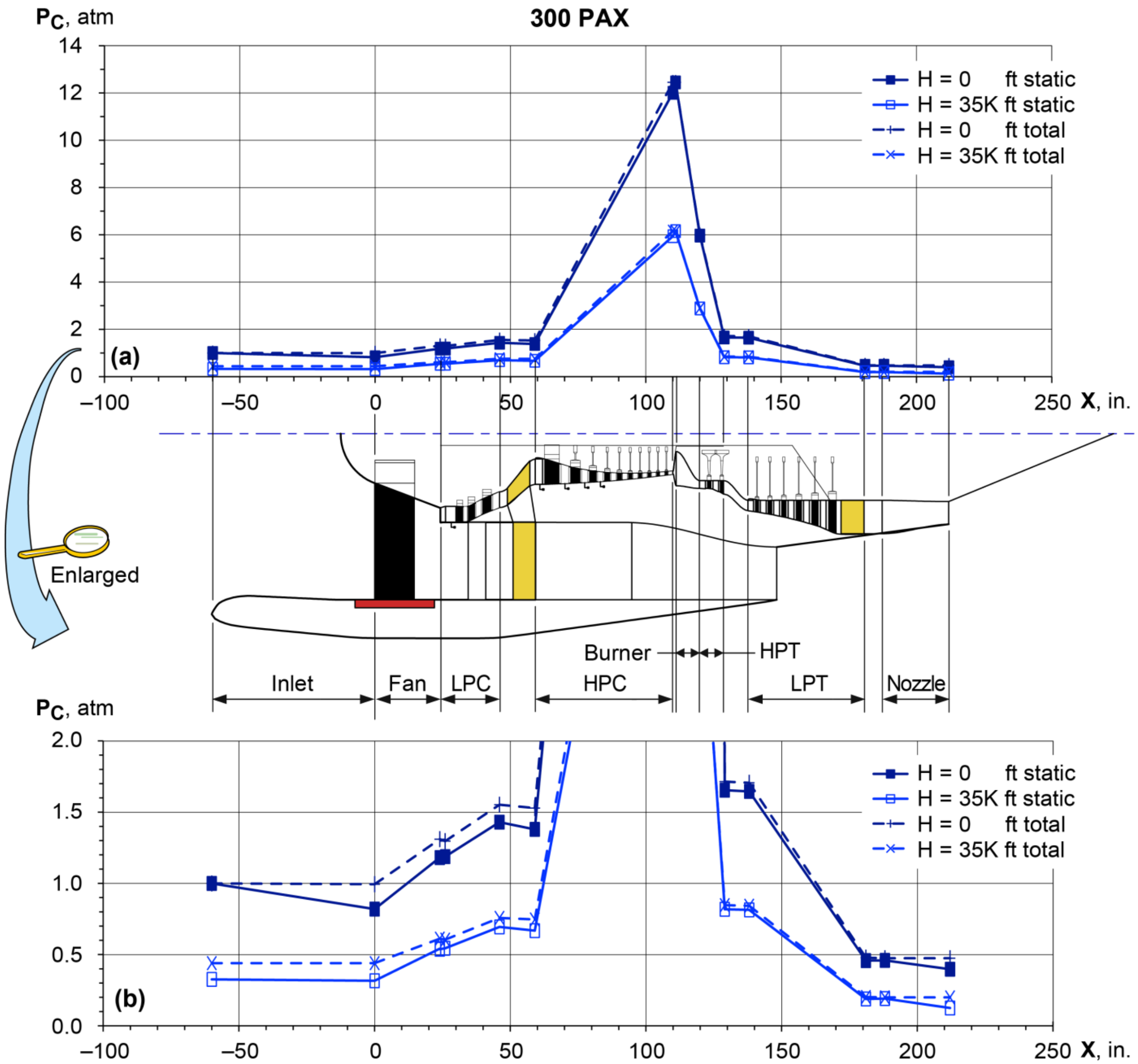

Figure 9a.—300 PAX engine–chamber pressure. (a) Full scale plot. (b) Enlargement of (a).

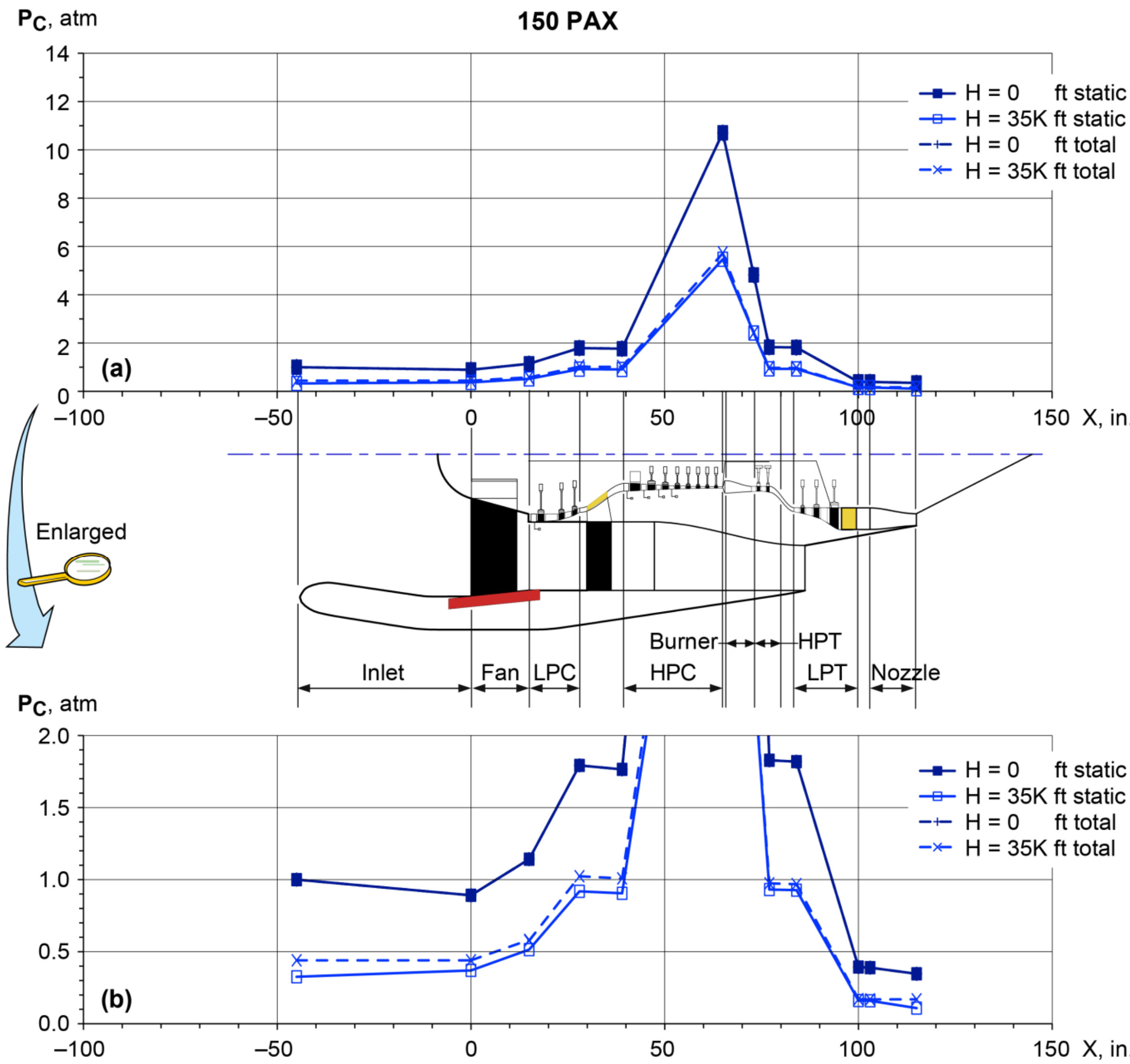

Figure 9b.—150 PAX engine–chamber pressure. (a) Full scale plot. (b) Enlargement of (a).

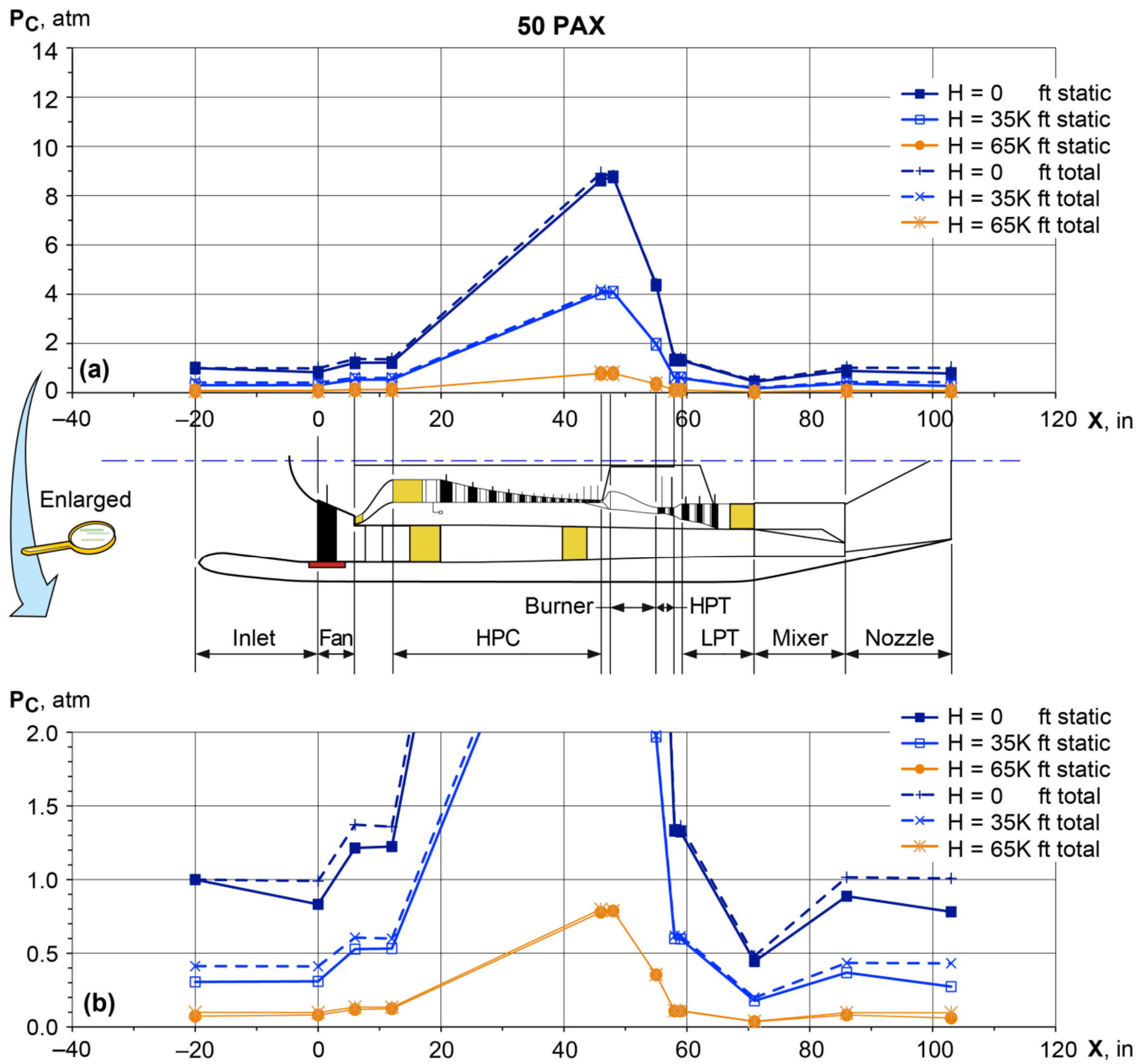

Figure 9c.—50 PAX engine–chamber pressure. (a) Full scale plot. (b) Enlargement of (a).

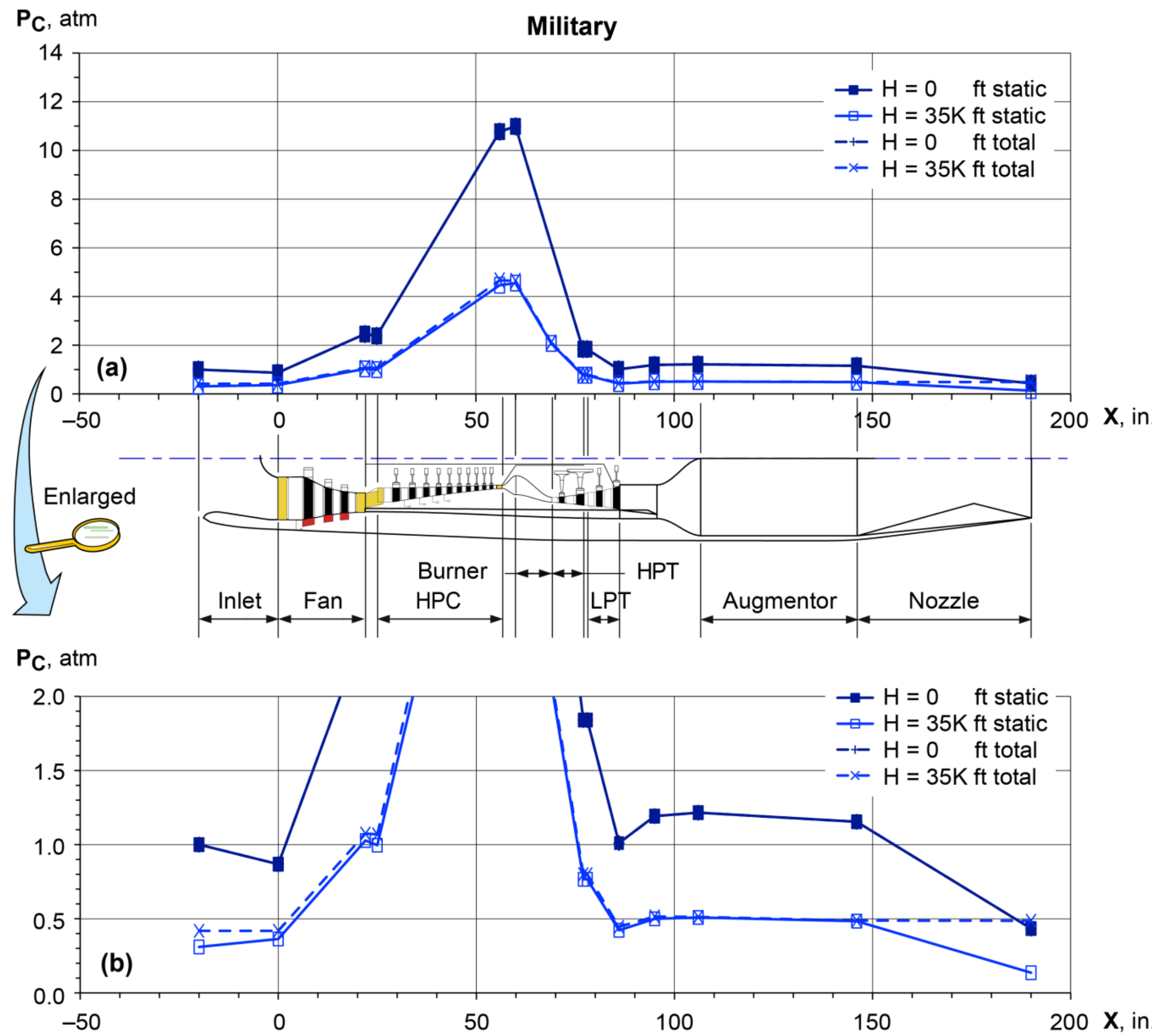

Figure 9d.—Military engine–chamber pressure. (a) Full scale plot. (b) Enlargement of (a).

REPORT DOCUMENTATION PAGE	*Form Approved* *OMB No. 0704-0188*

1. REPORT DATE *(DD-MM-YYYY)*	**2. REPORT TYPE**	**3. DATES COVERED** *(From - To)*
01-03-2011	Technical Memorandum	

4. TITLE AND SUBTITLE DBD Plasma Actuators for Flow Control in Air Vehicles and Jet Engines--Simulation of Flight Conditions in Test Chambers by Density Matching	**5a. CONTRACT NUMBER** **5b. GRANT NUMBER** **5c. PROGRAM ELEMENT NUMBER**
6. AUTHOR(S) Ashpis, David, E.; Thurman, Douglas, R.	**5d. PROJECT NUMBER** **5e. TASK NUMBER** **5f. WORK UNIT NUMBER** WBS 561581.02.08.03.21.13.02
7. PERFORMING ORGANIZATION NAME(S) AND ADDRESS(ES) National Aeronautics and Space Administration John H. Glenn Research Center at Lewis Field Cleveland, Ohio 44135-3191	**8. PERFORMING ORGANIZATION REPORT NUMBER** E-17602-1
9. SPONSORING/MONITORING AGENCY NAME(S) AND ADDRESS(ES) National Aeronautics and Space Administration Washington, DC 20546-0001 and U.S. Army Research Laboratory Adelphi, Maryland 20783-1145	**10. SPONSORING/MONITOR'S ACRONYM(S)** NASA, ARL **11. SPONSORING/MONITORING REPORT NUMBER** NASA/TM-2011-217006

12. DISTRIBUTION/AVAILABILITY STATEMENT
Unclassified-Unlimited
Subject Categories: 02, 05, 07, 13, and 75
Available electronically at http://www.sti.nasa.gov
This publication is available from the NASA Center for AeroSpace Information, 443-757-5802

13. SUPPLEMENTARY NOTES

14. ABSTRACT
Dielectric Barrier Discharge (DBD) Plasma actuators for active flow control in aircraft and jet engines need to be tested in the laboratory to characterize their performance at flight operating conditions. DBD plasma actuators generate a wall-jet electronically by creating weakly ionized plasma, therefore their performance is affected by gas discharge properties, which, in turn, depend on the pressure and temperature at the actuator placement location. Characterization of actuators is initially performed in a laboratory chamber without external flow. The pressure and temperature at the actuator flight operation conditions need to be simultaneously set in the chamber. A simplified approach is desired. It is assumed that the plasma discharge depends only on the gas density, while other temperature effects are assumed to be negligible. Therefore, tests can be performed at room temperature with chamber pressure set to yield the same density as in operating flight conditions. The needed chamber pressures are shown for altitude flight of an air vehicle and for jet engines at sea-level takeoff and altitude cruise conditions. Atmospheric flight conditions are calculated from standard atmosphere with and without shock waves. The engine data was obtained from four generic engine models; 300-, 150-, and 50-passenger (PAX) aircraft engines, and a military jet-fighter engine. The static and total pressure, temperature, and density distributions along the engine were calculated for sea-level takeoff and for altitude cruise conditions. The corresponding chamber pressures needed to test the actuators were calculated. The results show that, to simulate engine component flows at in-flight conditions, plasma actuator should be tested over a wide range of pressures. For the four model engines the range is from 12.4 to 0.03 atm, depending on the placement of the actuator in the engine. For example, if a DBD plasma actuator is to be placed at the compressor exit of a 300 PAX engine, it has to be tested at 12.4 atm for takeoff, and 6 atm for cruise conditions. If it is to be placed at the low-pressure turbine, it has to be tested at 0.5 and 0.2 atm, respectively. These results have implications for the feasibility and design of DBD plasma actuators for jet engine flow control applications. In addition, the distributions of unit Reynolds number, Mach number, and velocity along the engine are provided. The engine models are non-proprietary and this information can be used for evaluation of other types of actuators and for other purposes.

15. SUBJECT TERMS
Jet engines; Aeropropulsion; Turbomachinery; Compressor; Turbine; Gas turbine; Plasma; Dielectric barrier discharge; Flow control

16. SECURITY CLASSIFICATION OF:			**17. LIMITATION OF ABSTRACT**	**18. NUMBER OF PAGES**	**19a. NAME OF RESPONSIBLE PERSON**
					STI Help Desk (email:help@sti.nasa.gov)
a. REPORT	**b. ABSTRACT**	**c. THIS PAGE**			**19b. TELEPHONE NUMBER** *(include area code)*
U	U	U	UU	36	443-757-5802

Standard Form 298 (Rev. 8-98)
Prescribed by ANSI Std. Z39-18